BRILL

Insect Systematics & Evolution 50 (2019) 1-35

brill.com/ise

Phylogeny and evolution of the genus *Ctenocolum* Kingsolver & Whitehead (Coleoptera, Chrysomelidae, Bruchinae), with the description of three new species

Daiara Manfio[a], Isaac Reis Jorge[b], Gael J. Kergoat[c] and Cibele Stramare Ribeiro-Costa[b]

[a]Universidade Tecnológica Federal do Paraná (UTFPR), Campus Dois Vizinhos, Estrada para Boa Esperança, Km 04, Comunidade de São Cristóvão, 85660-000, Dois Vizinhos (PR), Brazil. E-mail: daiaramanfio@gmail.com

[b]Laboratório de Sistemática e Bioecologia de Coleoptera, Departamento de Zoologia, Universidade Federal do Paraná, Caixa Postal 19020, 81531-980, Curitiba, Paraná, Brazil. E-mail: isaac.r.jorge@gmail.com, cibele.ribeirocosta@gmail.com

[c]INRA - UMR CBGP (INRA, IRD, Cirad, Montpellier SupAgro), 755 Av. du campus Agropolis, 34988 Montferrier-sur-Lez, France. E-mail: gael.kergoat@inra.fr

Version of Record, published online 4 December 2017; published in print 2 January 2019

Abstract

The seed beetle genus *Ctenocolum* Kingsolver & Whitehead is peculiar because its preferred host *Lonchocharpus* Kunth (Fabaceae) is not preyed upon by other bruchine species. This study investigates the phylogenetic relationships and evolution of this genus and of its species groups, while providing the description of three new species and of the male of *C. biolleyi* Kingsolver & Whitehead. To infer phylogenetic relationships, a character matrix of 40 morphological characters was assembled and analysed using both parsimony and Bayesian inference. Ancestral state estimations of host plant use and biogeography analyses were also performed. A total of 22 species were examined: 16 *Ctenocolum* species (including the three new ones) and six outgroup bruchine species (from genera *Caryedes* Hummel, *Meibomeus* Bridwell, *Pygiopachymerus* Pic and *Pachymerus* Thunberg). All resulting trees support the monophyly of the genus *Ctenocolum*. Three synapomorphies characterize the genus: (i) head with frontal carina enlarged at base, (ii) male pygidium truncated apically, and (iii) lateral lobes of tegmen with dorsal process. The two known species groups are also recovered monophyletic in the parsimony analyses. The following three species are described: *Ctenocolum inmaculatus* Manfio & Ribeiro-Costa **sp. nov.** (Type locality: Venezuela, Guarico), which belongs to the group *tuberculatum*; *Ctenocolum nigronotus* Manfio & Ribeiro-Costa **sp. nov.** (Type locality: Porto Rico, Mayaguez) and *C. pallidus* Manfio & Ribeiro-Costa **sp. nov.** (Type locality: Republic of Guyana), which belong to the group *podagricus*. Finally, we present colored illustrations of dorsal patterns and male genitalia for these three new species and *C. biolleyi* in addition to an updated key for the genus *Ctenocolum*.

Keywords

Acanthoscelidina; Biogeography; Bruchinae; Host plants; new species; phylogenetic analyses; taxonomy; Western hemisphere

ZooBank: http://zoobank.org/E492E315-51F7-4E36-B000-D13F29A666FB

DOI 10.1163/1876312X-00002176

Introduction

The seed beetle *Ctenocolum* Kingsolver & Whitehead belongs to the group *Merobruchus* (Whitehead & Kingsolver 1975; Silva & Ribeiro-Costa 2008, but see Borowiec 1987 for an alternative arrangement) of the paraphyletic subtribe Acanthoscelidina (Kergoat et al. 2008) of tribe Bruchini. Distributed from the Nearctic region from Mexico to the Neotropical region (reaching Argentina), *Ctenocolum* is peculiar because its members are the only bruchine beetles that are known to consume seeds of *Lonchocarpus* Kunth, a genus of American plant of the tribe Millettieae (Fabaceae, Papilionoideae). This host plant genus is preferentially preyed upon by *Ctenocolum* species (17 *Lonchocarpus* species are known as hosts, which represent 70% of *Ctenocolum* known host plants). Consistent with the pattern of host use recovered in most seed beetle genera (see e.g. Kergoat et al. 2008), seeds of closely related genera (*Muellera* L. f. and *Piscidia* L.) are also consumed by *Ctenocolum* species (Albuquerque et al. 2014). These three Millettieae genera share the particularity of producing highly toxic rotenoids (deguelin and/or rotenone) secondary compounds (Bisby et al. 1994), which likely require specific detoxification pathways. The remaining known host plants of *Ctenocolum* are found in genera *Bauhinia* L. f. (Cercidoideae, Cercidae), *Dalbergia* L. f. (Papilionoideae, Dalbergieae), and *Peltophorum* (Vogel) Benth. (Caesalpinioideae, Caesalpinieae) (Albuquerque et al. 2014). With reference to the latter it is worth highlighting that rotenoids (rotenone) are also found in *Dalbergia* (Wink 2013).

Kingsolver & Whitehead (1974a), when describing the genus *Ctenocolum*, divided it into species groups, *podagricus* and *tuberculatum*. These groups were maintained in a recent taxonomic revision of the genus where five new species were described and placed in the exclusively Neotropical group *podagricus* (Albuquerque et al. 2014; Table 1). Following these descriptions, *Ctenocolum* comprises 13 species, nine of which are placed in the group *podagricus* while the remaining are placed in the group *tuberculatum*. In 1990, Kingsolver had estimated that 18 new species still had to be described in *Ctenocolum*. Between the three new species described in this paper and the five that have been described in the study of Albuquerque et al. (2014), only ten species descriptions are left before Kingsolver´s estimate is to be reached or exceeded. However, the diversity of the genus is likely even higher because of its wide distribution and the high level of diversity of potential host plants (for instance, the Millettieae encompasses 211 species of *Lonchocarpus*, three species of *Muellera* and eight species of *Piscidia*).

The number of phylogenetic studies on bruchines, although constantly increasing, is still low. Most of them have been only based on molecular data (but see Silvain & Delobel 1998 and Manfio et al. 2016) and more than 65% of studies have focused on the Palearctic and Paleotropical genera (Silvain & Delobel et al. 1998; Kergoat & Silvain 2004; Kergoat et al. 2004; Kergoat et al. 2005a; Tuda et al. 2006; Haines et al. 2007; Kergoat et al. 2007a, b; Kergoat et al. 2011; Delobel et al. 2013; Kergoat et al. 2015). The Western hemisphere, which encompasses the greatest number of seed beetle species (about 1000 species out of about 1650; Morse 2014), had its fauna sampled in only seven phylogenetic studies during the last 14 years (Nápoles et al. 2002; Kergoat et al. 2005b; Morse & Farrell 2005a, b; Alvarez et al. 2006; Kato et al.

2010; Manfio et al. 2013). Among the group *Merobruchus*, only the genus *Gibbobruchus* Pic had its monophyly recovered by a phylogenetic analysis (Manfio et al. 2013). Regarding *Ctenocolum*, a close relationship with genera *Caryedes* and *Meibomeus* has been postulated (Kingsolver & Whitehead 1974a, b; Whitehead & Kingsolver 1975; Borowiec 1987), however this hypothesis was exclusively intuitive, and it is not based on a phylogenetic analysis.

To increase our knowledge on the American genera of the paraphyletic Acanthoscelidina, in this study we investigate the phylogenetic relationships of the genus *Ctenocolum* and of its species groups based on analyses of a matrix of morphological characters. The resulting phylogenetic framework is then used to investigate the genus diversification with respect to host plant use and biogeography. We also provide the description of three new species and of the male of *Ctenocolum biolleyi* - previously unknown - along with illustrations and an updated key for *Ctenocolum* species.

Materials and Methods

Material Examined

The specimens examined and the type specimens are deposited in the USNM - United States National Museum of Natural History, Washington D.C., United States of America (A. Konstantinov and E. Roberts).

Morphological study

The methods used for morphological study and general terminology of the new species followed Albuquerque et al. (2014). The terms used for female genitalia rely on Lawrence et al. (2010) while the terms used to describe internal structures of male genitalia follow Kingsolver (1970). Here the term "squamous sclerite" described in Albuquerque et al. (2014) was changed to "squamous structure" as we do not think that this structure and the sclerotized sclerite named "smooth sclerite" by the same authors are homologous. Colored images of external morphology were obtained with sequential images mounting at different focal planes with a LEICA MZ16 stereomicroscope, a LEICA DFC 500 camera, and two LEICA modules (LAS 3D VIEW and LAS MONTAGE). Images of male genitalia were obtained using a Sony Cyber-Shot DSC W350 digital camera coupled with an Olympus BX50 optical microscope. Measurements were done with the software AxioVision Rel 4.8 over images captured with the Sony Cyber-Shot DSC W350 digital camera coupled in the stereoscopic microscope Leica M165C. Diagnoses followed the definition of the International Code of Zoological Nomenclature - ICZN (1999). The descriptions follow the practices described by Ratcliffe (2013), except for terms referring to integument and pubescence characters, which follow recent studies on Bruchinae (Albuquerque et al. 2014; Manfio & Ribeiro-Costa 2016). For the type label data, double quotes (‘ ’) separate different labels, each of which are enumerated in parentheses from uppermost to lowermost for type and non-type specimens; and slashes (/) separate different lines in the same label.

Table 1. *Ctenocolum* and its species groups.

Groups	Species
Group *podagricus*	*C. aquilus* Albuquerque & Ribeiro-Costa, 2014
	C. biolleyi Kingsolver & Whitehead, 1974
	C. colburni Kingsolver & Whitehead, 1974
	C. martiale Kingsolver & Whitehead, 1974
	C. milelo Albuquerque & Ribeiro-Costa, 2014
	C. podagricus (Fabricius, 1801)
	C. punctinotatus Albuquerque & Ribeiro-Costa, 2014
	C. pygospilotus Albuquerque & Ribeiro-Costa, 2014
	C. triangulatus Albuquerque & Ribeiro-Costa, 2014
Group *tuberculatum*	*C. acapulsensis* Kingsolver & Whitehead, 1974
	C. janzeni Kingsolver & Whitehead, 1974
	C. salvini (Sharp, 1885)
	C. tuberculatum (Motschulsky, 1874)

The abbreviations used were: BL, body length (from anterior margin of pronotum to elytra apex) and BW, body width (the largest width on the subapical region of the elytra).

Phylogenetic analyses

Phylogenetic inference analyses were performed on a dataset comprising 22 terminal taxa. As ingroups, in addition to the three new *Ctenocolum* species that we describe here, we used the 13 species of *Ctenocolum* recognized as valid in the taxonomic revision of the genus (Albuquerque et al. 2014) and belonging to two species groups (Table 1).

Outgroups consisted of *Caryedes brasiliensis* (Thunberg), *Caryedes godmani* (Sharp), *Meibomeus funebris* (Boheman), *M. petrolinae* Silva & Ribeiro-Costa and *Pygiopachymerus lineola* (Chevrolat), specimens from genera intuitively closer to *Ctenocolum* (Kingsolver & Whitehead 1974a, b, Whitehead & Kingsolver 1975, Borowiec 1987). In addition, *Pachymerus bactris* L. from a distinct bruchine tribe (Pachymerini) was included to root the tree.

Morphological characters retained for phylogenetic analyses encompass both external and internal (male and female genitalia) characters, in accordance with those previously highlighted in Albuquerque et al. (2014). Most of characters were coded as binary. When necessary we used "contingent coding" to avoid multistate characters (Forey & Kitching 2000). The matrix was constructed in Mesquite v. 2.75 (Maddison & Maddison 2015). Missing data were coded as '?' and inapplicable states as '-'. The resulting matrix was then analyzed using both parsimony and Bayesian inference.

Parsimony analyses were conducted on the unweighted character data set using TNT ver. 1.1 (Goloboff et al. 2008). Heuristic searches were conducted using the following parameters: "Max.tree" = 10000; "random seed" = 1; "number of additional sequences" = 1000; "tree to save per replication" = 10; and tree bisection reconnection (TBR) as

branch swapping algorithm; the option "collapse tree after the search" was marked to avoid trees having branches without support were saved in the memory. Branch support was investigated using Bremer support (BS) values (Bremer 1994) and bootstrap symmetric resampling (Goloboff et al. 2003). Because of the lack of clear statistical interpretations for the BS (Debry 2001), we used the arbitrarily threshold of 4 proposed by (Felsenstein 1985) to identify well-supported nodes using BS values. For symmetric resampling values, the standard threshold of 70% for bootstrap values (BV) (Hillis & Bull 1993) was used. To represent the resulting cladograms we used Winclada ver. 0.9.9 (Nixon 1999).

Bayesian inference analyses were carried out on the morphological dataset using MrBayes 3.2.3 (Ronquist et al. 2012). To analyse the morphological dataset under Bayesian inference we used the maximum likelihood model for discrete morphological character data (Markov *k* or Mk) of Lewis (2001). Inapplicable character states were treated as missing data. We conducted two independent runs with eight Markov Chains Monte Carlo (one cold and seven incrementally heated) that ran for 50 million generations, with trees sampled every 1,000 generations. A conservative burn-in of 25% was then applied after checking for stability on the log-likelihood curves and the split-frequencies of the runs. Support of nodes for MrBayes analyses was provided by clade posterior probabilities (PP) as directly estimated from the majority-rule consensus topology. Nodes supported by PP ≥ 0.95 were considered strongly supported following Erixon et al. (2003). Whenever a group of interest was recovered in paraphyly, we used Bayes factors (B_F) to assess whether there was statistical support for their non-monophyly. To do so, specific analyses (in which taxa of interest are constrained to be monophyletic) were carried out using MrBayes.

To examine hypotheses concerning the evolution of host associations and biogeography we carried out parsimony reconstructions of ancestral states using Mesquite 3.2 (Maddison & Maddison 2017). For these analyses the strict consensus tree from the parsimony analysis was used as a guide tree. Host plant associations were coded according to established associations with host genera while biogeographic distributions were categorized according to Morrone (2014). All corresponding data is summarized in Tables 2 and 3.

Results and Discussion

Phylogenetic analyses

A total of 40 morphological informative characters were defined from adult: 22 from external morphology (1–22), 18 from male genitalia (23–39), and 1 from female terminalia (40) (see Table 4). The complete matrix is shown in Appendix 1.

The parsimony analysis using equal weighting generated three equally parsimonious trees (length, L = 76; Consistency Index, CI = 0.59; Retention Index, RI = 0.81). Based on these three equally parsimonious topologies we inferred a strict consensus

Table 2. *Ctenocolum* and its hosts plants association.

***Ctenocolum* species/ Host plant**	**Group *podagricus***											**Group *tuberculatum***					
	C. aquilus	*C. biolleyi*	*C. colburni*	*C. martiale*	*C. milelo*	*C. nigronotus* **sp. n.**	*C. palidus* **sp. n.**	*C. podagricus*	*C. punctinotatus*	*C. pygospilotos*	*C. triangulatus*	*C. acapulcensis*	*C. inmaculatus* **sp. n.**	*C. janzeni*	*C. salvini*	*C. tuberculatum*	Total
Schnella glabra (=*Bauhinia glabra*)								**g**									1
Dalbergia retusa															**f**		1
Dahlstedtia muehlbergiana (=*L. muehlbergianus*)	**h**				**g**												2
Lonchocarpus constrictus				**c**													1
L. costaricensis								**e, f, d**				**g**				**e, f, c, d**	3
L. cultratus (=*L. guillemineanus*)					**g**												1
L. emarginatus														**g**			1
L. eriocarinalis		**e, f**		**c**								**e, f, c**					3
L. hondurensis								**c**									1
L. latifolius (=*L. heptaphyllus*)			**c**					**c**									2
L. longistylus																**c**	1
L. macrocarpus (=*L. margaritensis*)								**c**									1
L. minimiflorus								**e, d**								**e, d**	2
L. nitidus								**f, c**						**i**		**f**	3
L. parviflorus								**f**								**f**	2
L. purpureus			**c**														1
L. rugosus								**e, c**						**j**		**e**	3
L. sericeus				**c**				**NR**									1
L. velutinus			**f**														1
Muellera sp.							**NRG**										1
Peltophorum gasyrrhachis								**c***									1
Piscidia carthagenensis								**e, f, c, d**						**e, f, c**			2
Piscidia grangifolia														**c**			1
Piscidia mollis														**c, g**			1
Piscidia piscipula						**NR**		**a, b, c**		**k**				**l**			4
Total	1	1	3	3	2	1	1	12	0	1	0	2	0	7	1	6	

Synonym of *L. cultratus, L. latifolius* and *L. macrocarpus* in Silva & Tozzi, 2012; Combination of *Dahlstedtia muehlbergiana* in Silva et al., 2012; Combination of Schnella glabra in Wunderlin, 2010; (NR) new record; (NRG) new record for the genus; (?) dubious insect identification (a) Zacher, 1952; (b) de Luca, 1972; (c) Kingsolver & Whitehead, 1974; (d) Janzen, 1975; (e) Janzen, 1977, 1978; (f) Janzen, 1980; (g) Hetz & Johnson, 1988 (h) Sari et al., 2002; (i) Romero & Johnson, 2002; (j) Romero & Westcott, 2011; (k) Albuquerque et al., 2014; (l) Nápolis, 2016.

Table 3. *Ctenocolum* host plants association and geographic distribution included the biogeographic areas of Morrone (2014).

Species group	Species	Distribution
Group *podagricus*	*C. aquilus*	Chacoan subregion: Brazil (São Paulo, Paraná).
	C. biolleyi	Brazilian subregion: Costa Rica (Puntarenas Province, San Jose).
	C. colburni	Brazilian subregion: Mexico (Veracruz), Guatemala (Chimaltenango), Honduras (Colón, Copán, El Paraíso), Costa Rica (Heredia).
	C. martiale	Brazilian subregion: Mexico (Nayarit, Jalisco, Veracruz, Michoacán, Guerrero, Oaxaca), Trinidad and Tobago (Trinidad).
	C. milelo	Chacoan subregion: Bolivia (Santa Cruz), Brazil (São Paulo).
	C. nigronotus **sp. n.**	Brazilian subregion: Puerto Rico (Mayaguez).
	C. palidus **sp. n.**	Brazilian subregion: Republic of Guyana.
	C. podagricus	Antillean subregion: Dominican Republic (Dajabom), Jamaica (Saint James). Brazilian subregion: Puerto Rico, Mexico (Sinaloa, Jalisco, Querétaro, Veracruz, Chiapas, Campeche, Tabasco, Quintana Roo), Guatemala, El Salvador (San Salvador, La Unión), Nicaragua, St. Barthelemy, Costa Rica (Guanacaste, Puntarenas), Trinidad and Tobago (Tobago), Venezuela (Distrito Federal), Ecuador, Guyana, Peru (Junin), Brazil (Rondonia). Chacoan subregion: Brazil (Mato Grosso, Paraná), Bolivia, Paraguay, Argentina.
	C. punctinotatus	Brazilian subregion: Ecuador (Guayas).
	C. pygospilotos	Nearctic region: United States Virgin Islands.
	C. triangulatus	Brazilian subregion: Colombia.
Group *tuberculatum*	*C. acapulcensis*	Brazilian subregion: Mexico (Jalisco, Guerrero), Costa Rica (Guanacaste).
	C. inmaculatus **sp. n.**	Brazilian subregion: Venezuela (Guarico).
	C. janzeni	Nearctic region: Mexico (Sonora, Tamaulipas). Antillean subregion: Dominica. Brazilian subregion: Mexico (Sinaloa, San Luis Potosí, Jalisco, Michoacan, Veracruz, Morelos, Oaxaca, Chiapas), Guadeloupe, Honduras (Olancho), Costa Rica (Guanacaste, Puntarenas).
	C. salvini	Brazilian subregion: Guatemala (Sacatepéquez).
	C. tuberculatum	Brazilian subregion: Mexico (Nayarit, Jalisco, Oaxaca, Yucatán), Guatemala (Escuintla), Honduras (Olancho), Costa Rica (Guanacaste), Panama, Venezuela (Aragua).

tree (Figure 1A). Discussions on results of parsimony analyses refer to this strict consensus tree (length, L = 78 steps; Consistency Index, CI = 0.53; Retention Index, RI = 0.80). Overall, the clade support is low with only two nodes exhibiting Bremer indices ≥ 4 and three nodes exhibiting bootstrap symmetric resampling values (BV) ≥ 70%.

The unconstrained Bayesian inference analyses yield a consensus tree (Figure 2) associated with a mean harmonic mean score of –280.229. In comparison to the results of the parsimony analyses, the clade support is slightly higher with five nodes supported by PP ≥ 0.95.

Table 4. List of characters and character states used for the phylogeny of *Ctenocolum,* and parsimony reconstruction of ancestral states of host plant associations and biogeography. Note that host plant and biogeography was not used in phylogeny reconstruction.

	HEAD
1	*Frontal carina, base:* (0) straight (Figure 5); (1) enlarged, forming a triangle (Figures. 15, 23, 30).
2	*Eye, number of facets behind ocular sinus:* (0) from 3 to 5 (Figures. 15, 23, 30); (1) more than 8 (Figure 5).
	THORAX
3	*Pronotum, subbasal gibbosity:* (0) absent; (1) present (Figure 6).
4	*Pronotum, median gibbosity, transversal sulcus:* (0) absent (Figure 36); (1) present (Figure 14).
5	*Pronotum, lateral marginal line:* (0) absent; (1) present.
6	*Pronotum, lateral carina:* (0) absent; (1) presente (Figure 6, 7).
7	*Pronotum, lateral carina, length:* (0) about half of pronotum, never reaching cervical sulcus (Figure 6); (1) reaching cervical sulcus (Figure 7).
8	*Metaventrite:* (0) plane, not protuberant; (1) protuberant (Figure 8).
9	*Elytron, striae 3-5, basal tubercle:* (0) absent; (1) present.
10	*Elytron, stria 3, denticle:* (0) absent; (1) present.
11	*Elytron, stria 4, denticle:* (0) absent; (1) present.
12	*Elytron, stria 6, punctuation, distribution:* (0) on the entire extension; (1) restricted to base..
13	*Hind leg, femur, greatest width in relation to the greatest width of the coxa:* (0) less than or about equal; (1) more than 1.5 times (Figures. 14, 22, 29).
14	*Hind leg, femur, external ventral margin, toothed carina:* (0) absent; (1) present (Figure 9).
15	*Hind leg, femur, above external ventral margin, denticles:* (0) absent; (1) present (Figure 9).
16	*Hind leg, tibia, curvature:* (0) on apical third to half (Figures. 8, 36); (1) entirely arcuate (Figure 14).
17	*Hind leg, tibia, outer surface, texture of integument:* (0) smooth, without row of denticles; (1) with row of denticles (Figure 9).
18	*Hind leg, tibia, length of mucro in relation to the width of tibia at apex:* (0) less than half; (1) more than half (Figure 29); (2) equal or more than apex (Figures. 8, 14).
19	*Hind leg, tibia, apical border, lateral coronal tooth:* (0) absent (Figures. 9, 14); (1) present (Figure 29).
20	*Hind leg, length of basitarsus in relation to length of tibia:* (0) up to 1/3; (1) half or more (Figure 8).
21	*Hind leg, basitarsus, lateral carina:* (0) absent; (1) present (Figure 8).
	ABDOMEN
22	*Pygidium, apex (male):* (0) rounded; (1) truncated (Figure 24, 38).
	MALE GENITALIA
23	*Median lobe, ventral valve, apex: (*0) rounded (Figure 17); (1) truncated (Figures. 25, 32, 40).
24	*Median lobe, ventral valve:* (0) continuous to the tubular region (Figure 12); (1) articulated to the tubular region (Figures. 10, 17, 25, 32, 40).
25	*Median lobe, ventral valve, basal margin:* (0) not emarginated; (1) emarginated (Figure 40).
26	*Median lobe, dorsal valve, format:* (0) triangulated (Figure 12); (1) rounded.
27	*Median lobe, length in relation to the width on median line:* (0) up to 6.5 times (Figures. 12, 17, 25, 32, 40); (1) more than 8.5 times (Figure 10).
28	*Median lobe, tubular region, apical half, fracture:* (0) absent (Figures. 12, 17, 25, 32, 40); (1) present (Figure 10).

29 *Median lobe, internal sac, apex (behind the ventral valve), median tuft of spicules:* (0) absent (Figure 10); (1) present (Figure 32).
30 *Median lobe, internal sac, submedian region, smooth sclerite:* (0) absent; (1) present (Figure 17).
31 *Median lobe, internal sac, submedian region, squamous structure:* (0) absent; (1) present (Figures. 25, 32, 40).
32 *Median lobe, internal sac, hinge sclerite:* (0) absent; (1) present (Figure 17).
33 *Tegmen, lateral lobes, apical margin, tooth:* (0) absent; (1) present (Figure 34).
34 *Tegmen, lateral lobes, apical margin, tooth, format:* (0) obtuse (Figure 40).; (1) acute (Figure 34).
35 *Tegmen, lateral lobes, emargination in relation to the length of lateral lobes:* (0) shallow, from 0.04 to 0.1 times (Figure 11); (1) deep, from 0.5 to 0.8 times (Figures. 18, 26, 34, 41).
36 *Tegmen, lateral lobes deeply emarginated, greatest width of apex in relation to the smallest width in median line of one lobe:* (0) about equal; (1) expanded, from 2 to 5.5 times (Figure 18).
37 *Tegmen, lateral lobes, dorsal region, base, process:* (0) absent; (1) present (Figure 27).
38 *Tegmen, strut, keel:* (0) absent (Figure 9); (1) present (Figure 18, 26–27, 34, 41).
39 *Tegmen, strut, keel, position:* (0) only dorsal; (1) dorsal and ventral (Figure 27).

FEMALE TERMINALIA

40 *VIII sternite, length from the apex to the spiculum ventrale insertion in relation to the width on median region:* (0) wider than long (Figure 43).; (1) longer than wide (Figure 42).

HOST PLANT

41 *Host plant genus association:* (0) Cercidoideae - Bauhiniinae - *Schnella*; (1) Papilionoideae - Dalbergieae - *Dalbergia*; (2) Papilionoideae - Clitoriinae - *Centrosema*; (3) Papilionoideae - Core-Millettieae - *Piscidia*; (4) Papilionoideae - Core-Millettieae - *Muellera*; (5) Papilionoideae - Core-Millettieae - D*ahltedtia*; (6) Papilionoideae - Core-Millettieae - *Lonchocarpus*; (7) Papilionoideae - Diocleae - *Dioclea*; (8) Papilionoideae - Desmodiae - *Desmodium*.
42 *Biogeographic regionalisation:* (0) Nearctic; (1) Antillean Subregion; (2) Brazilian subregion; (3) Chacoan Subregion.

Both parsimony and Bayesian inference analyses recover a monophyletic genus *Ctenocolum* (BS of 3, BV of 68%, PP of 0.96). Under parsimony *Ctenocolum* is recovered as sister to a clade grouping *Caryedes* + *Meibomeus*, but with a weak support (BS of 1, BV of 39%) (Figure 1A). These three genera share five synapomorphies: stria 6 of elytra punctate only at base (12(1); Figures 13, 25, 21, 35); metabasitarsus half or more than length of tibia (20(1); Figure 8); ventral valve articulated to the tubular region (24(1); Figures 10, 17, 25, 32, 40) and rounded at apex (26(1)); internal sac with hinge sclerites (32(1); Figure 17). Under Bayesian inference *Ctenocolum* is recovered as sister to *Pygiopachymerus*, but again this placement is weakly supported (PP of 0.55) (Figure 2). All *Ctenocolum* species form a relatively well-supported lineage (BS of 3, BV of 68%, PP of 0.96), also characterized by three synapomorphies, respectively: head with frontal carina enlarged at base (1(1); Figures 15, 23, 30); male pygidium truncated apically (22(1); Figures 24, 38); lateral lobes of tegmen with dorsal process (37(1) Figure 27).

Under parsimony two main clades of *Ctenocolum* are recovered (Figure 1A). It is not the case under Bayesian inference, where three distinct lineages can be distinguished

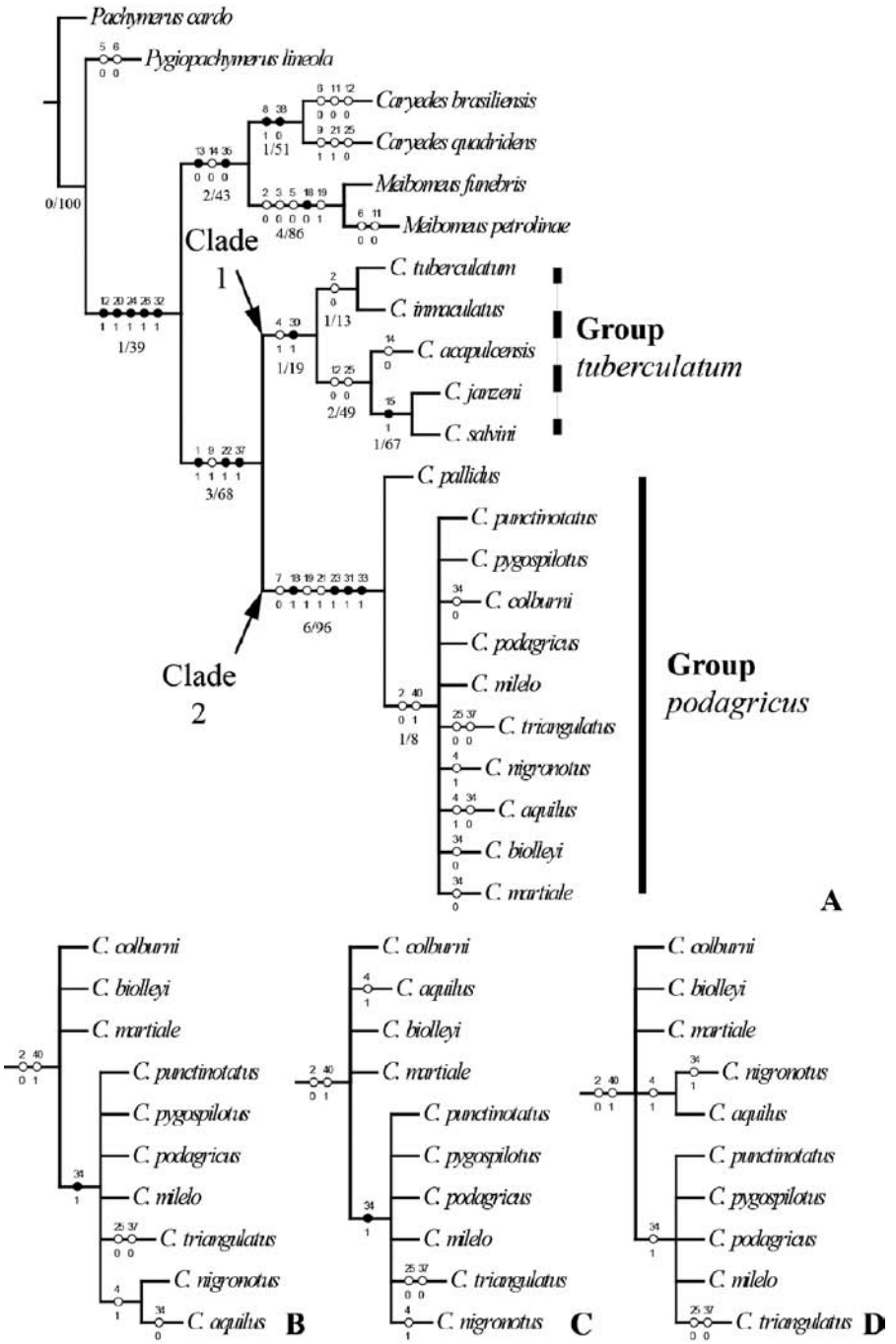

Fig. 1. A Strict consensus of the three most parsimonious trees based on a parsimony analysis of the morphological dataset (78 steps, CI = 0.53, RI = 0.80). Filled circles represent unique changes, open circles represent multiple changes. Values for the Bremer (BS) and symmetric resampling (BV) support are below branches. B–D. Three different equiparsimonious hypotheses.

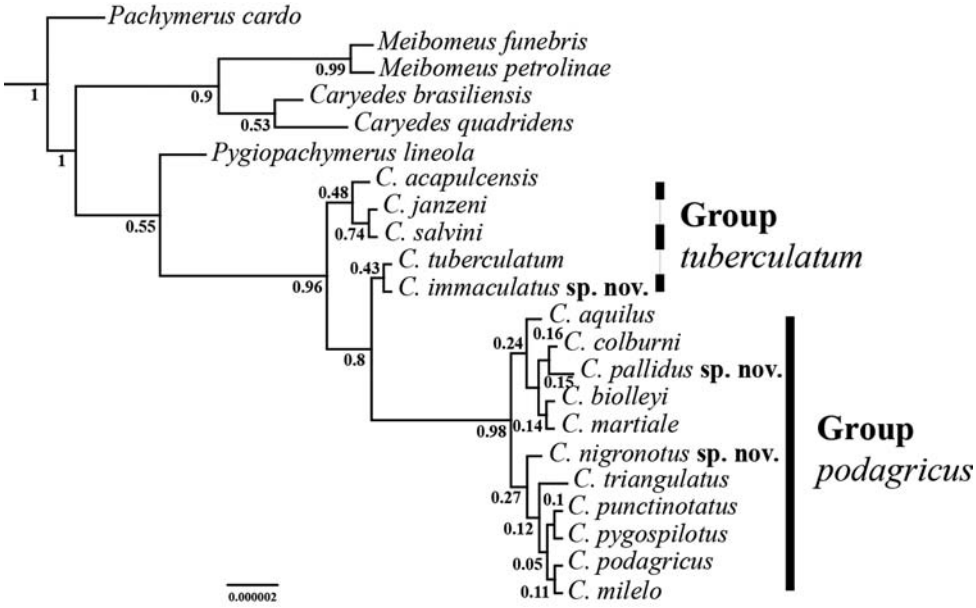

Fig. 2. Bayesian inference consensus topology based on the analysis of the morphological dataset. Branch support is figured on nodes using PP.

(Figure 2). Here it is worth underlining that additional analyses in which *Ctenocolum* are constrained into two distinct clades (similar to those inferred under parsimony) yield a mean harmonic mean estimate of –281.353 versus –280.229 for the unconstrained analyses. Hence the difference corresponds to a statistically non-significant B_F of 2.248, below the standard threshold of 10 advocated by Kass & Raftery (1995). Therefore, the Bayesian inference analyses cannot exclude the hypothesis supported by the parsimony analyses regarding the existence of two distinct *Ctenocolum* lineages.

A first clade (referred as Clade 1 in Figure 1A) is composed of five species ((*C. tuberculatum* (Motschulsky) + *C. inmaculatus*) + *C. acapulcensis* Kingsolver & Whitehead (*C. janzeni* Kingsolver & Whitehead + *C. salvini* (Sharp))) sharing one synapomorphic character, the presence of a smooth sclerite on male genitalia (30(1); Figure 17), and one homoplasious character, the median gibbosity of pronotum with transversal sulcus (4(1), a character state shared with *C. aquilus* Albuquerque & Ribeiro-Costa and *C. nigronotus*; Figure 14). Inside this clade, *C. tuberculatum* + *C. inmaculatus* have in common the fact that they have a few number of facets behind ocular sinus (2(0), a character state shared with species of *Meibomeus* and other *Ctenocolum* species; Figures 15, 23, 30). The other three species in this clade, *C. acapulcensis* (*C. janzeni* + *C. salvini*) have in common two homoplasies: the stria 6 of elytra entirely punctuated (12(0); a character state unique inside *Ctenocolum*; Figure 4) and the ventral valve of male genitalia not emarginated at basal margin (25(0), a character state shared with *C. triangulatus* Albuquerque & Ribeiro-Costa and the outgroup *Caryedes quadridens*). *Ctenocolum janzeni* + *C. salvini* appear as sister because they share the following synapomorphic character state: hind femur with denticles above external ventral margin (15(1); Figure 9).

The other major *Ctenocolum* clade (referred to as Clade 2 in Figure 1A) is well supported in all analyses (BS of 6, BV of 96%, PP of 0.98); it includes the remaining eleven species of *Ctenocolum* and is characterized by four synapomorphies and three homoplasious character states, as follows: hind tibia, mucro more than half width of tibia at apex (18(1); Figure 29); ventral valve truncate at apex (23(1); Figures 25, 32, 40); internal sac of male genitalia with squamous sclerite (31(1); Figures 25, 32, 40); lateral lobes of tegmen with a tooth on apical margin (33(1); Figures 34A, 41A); lateral carina of pronotum about half of pronotum (7(0), shared only with *M. funebris*); hind tibia with lateral coronal tooth (19(1), shared with the species of *Meibomeus*; Figure 29); and, metabasitarsus with lateral carina (21(1), shared only with *Caryedes quadridens*; Figure 8). Under parsimony, *C. pallidus* is found sister to the remaining 10 species (Figure 1A), but with a really low support (BS of 1, BV of 8%). There are three possible alternative phylogenetic hypotheses within these 10 species (*C. punctinotatus* Albuquerque & Ribeiro-Costa + *C. pygospilotus* Albuquerque & Ribeiro-Costa + *C. colburni* Kingsolver & Whitehead + *C. podagricus* (Fabricius) + *C. milelo* Albuquerque & Ribeiro-Costa + *C. triangulatus* Albuquerque & Ribeiro-Costa + *C. nigronotus* + *C. aquilus* + *C. biolleyi* + *C. martiale* Kingsolver & Whitehead) based on the trees that have been used to generate the consensus tree (Figures 1B-D). Among these, we point to a character not described in the previous study, the presence of an acute tooth on apical margin of lateral lobes (34(1); Figure 34A), which constitutes a synapomorphy for *C. punctinotatus* + *C. pygospilotus* + *C. podagricus* + *C. milelo* + *C. triangulatus* + *C. nigronotus* (Figures 1B, C). Under Bayesian inference, *C. pallidus* is recovered in a more derived position (sister to *C. colburni*); however all relationships within the clade are unsupported (all PP are below 0.3).

Among the genera of the group *Merobruchus*, *Ctenocolum* was considered as part of "*Caryedes* assemblage" with *Caryedes* and *Meibomeus* because of relatively elongated frons, elongated gena and antennal scrobe of gena equal to or larger than the diameter of antennal fossa, abdomen and pygidium lacking glabrous polished areas (Kingsolver & Whitehead 1974a; Whitehead & Kingsolver 1975; Borowiec 1987). Although we did not include these characters in the present study because they were not possible to codify, our results corroborates the hypothesis reported in the literature thanks to the new characters we selected.

Albuquerque et al. (2014) pointed out some characters that in combination separate *Ctenocolum* from *Caryedes* and *Meibomeus*, such as: striae 3 and 4 curved at base and each with a tooth (characters 10(1) and 11(1), not exclusive of *Ctenocolum*); very enlarged femur about 1.5 times the width of hind coxa (character 13(1); Figures 14, 22, 29); larger number of teeth on pecten, 6–18 (character not used because of its subjectivity and polymorphism but it is unquestionable that *Ctenocolum* has usually more tooth on its pecten in comparison with other closely related genera); mucro shorter than apical width of tibia (we reinterpreted this character and concluded that the species of the Clade 1 (Figure 1A), considered with a short mucro by Albuquerque et al. (2014) have a long mucro, equal or longer than apex of tibia (18(2); Figures 8, 14); short median lobe (27(0), shared with *P. lineola*; Figures 12, 17, 25, 32, 40) without fracture before apex (28(0), not exclusive of *Ctenocolum*; Figures 12, 17, 25, 32, 40);

internal sac with hinge sclerites (32(1), a synapomorphy to *Ctenocolum*, *Caryedes* and *Meibomeus*; Figure 16) and other sclerites (smooth sclerite, 30(1); Figures 25, 32, 40 and, squamous sclerite here named squamous structure, 31(1); Figure 17); tegmen with lateral lobes deeply emarginated (35(1), shared with *P. lineola*; Figures 18, 26, 34, 41).

In *Ctenocolum*, the two species groups intuitively proposed by Kingsolver and Whitehead (1974a) and maintained in the taxonomic revision of Albuquerque et al. (2014) are hereby recovered monophyletic under parsimony; these two groups also cannot be discarded based on the results of the Bayesian inference analyses. The group *tuberculatum* is consistent with the Clade 1 in the present parsimony study (Figure 1A). The species of this group stands out among other *Ctenocolum* - and even in relation to the other genera of the group *Merobruchus* sampled here - mainly because of the presence of the large sclerite in the male genitalia (30(1), smooth sclerite; Figure 17). Kingsolver and Whitehead (1974a) remarked that the large, symmetric and complex sclerite on the male genitalia could be putative evidence that the group *tuberculatum* could be a natural group, which was corroborated by our phylogenetic analysis. Besides this character, others were used to diagnose the group *tuberculatum* for instance lateral carina reaching cervical sulcus (7(1); Figure 7), hind femur with second tooth of pecten regular in profile until apex (it was not possible to test this character), with row of denticles in the outer surface (17(1); Figure 9), apex without lateral coronal tooth (19(0); Figures 9, 14), 1-tarsomere without lateral carina (21(0); Figure 8), all shared with outgroup taxa (Albuquerque et al. 2014). With respect to the internal relationships, it was also corroborated that *C. acapulcensis*, *C. salvini* and *C. janzeni* are closer to each other than to *C. tuberculatum*, as suggested in the literature (Kingsolver & Whitehead 1974a; Albuquerque et al. 2014).

The group *podagricus* is consistent with the Clade 2 recovered in all our phylogenetic analyses (Figures 1A, 2). As previously indicated, this group is well-characterized by eight synapomorphic and homoplasious characters, all quoted by Albuquerque et al. (2014; pg. 17) in the diagnosis of the group, except: length of hind mucro more than a half width of tibia at apex (18(1); Figure 29), a character state that was reinterpreted here; and lateral lobes of tegmen with tooth on apical margin (33(1); Figures 34A, 41A), a character never described before. Kingsolver and Whitehead (1974a) mentioned that the group *podagricus* probably is a natural group, but the relationships among its species are not clear. Through our analysis we corroborated with both Kingsolver and Whitehead (1974a) assumptions regarding the monophyly of the group *podagricus*.

Ancestral state estimation and biogeographic analyses

A clear pattern of phylogenetic conservatism of host use was inferred at the tribe level on Millettieae (Figure 3). Such level of conservatism in host use is consistent with those recovered in other seed-beetle groups (e.g. Kergoat et al. 2008). Plants belonging to the genus *Lonchocarpus* are preferentially fed upon by *Ctenocolum* species; the diet of some species also includes other related genera in the Millettieae such as *Dahlstedtia*

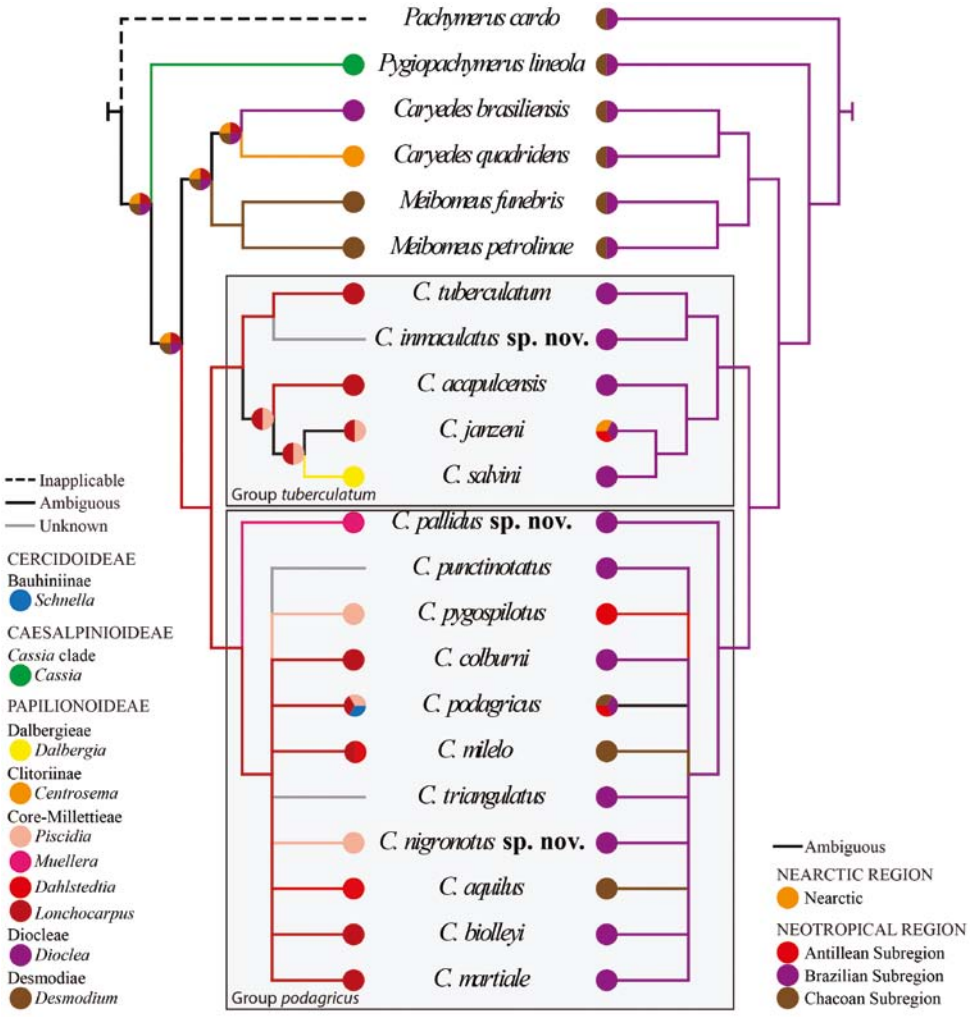

Fig. 3. Ancestral state estimation and biogeographic analyses using as a guide tree the strict consensus tree from the parsimony analysis of the morphological dataset. On the evolution of host plant use is presented while reconstruction of ancestral geographic areas is figured on the right. Detailed legends for both character optimizations are shown on the top of the figure.

Malme, *Muellera* and *Piscidia* (Table 2, Figure 3). These four plant genera belong to a subclade of the 'core-Millettieae clade' (*sensu* Hu et al. 2002), which differs from other Millettieae by the lack of *L*-Canavanine (Schrire 2005). Three *Ctenocolum* species exhibit wider host ranges: *Ctenocolum podagricus* (12 host plant species, mostly in the genus *Lonchocarpus*), *C. janzeni* (seven host plant species, mostly in the genus *Piscidia*) and *C. tuberculatum* (six host plant species, all belonging to the genus *Lonchocarpus*) (Table 2). Ancestral state estimation analyses suggest an ancestral association of the genus *Ctenocolum* with *Lonchocarpus* hosts (Figure 3). Expansion of host-range was inferred for three species: *C. janzeni* (on *Piscidia*), *C. milelo* (on *Dahlstedtia*) and

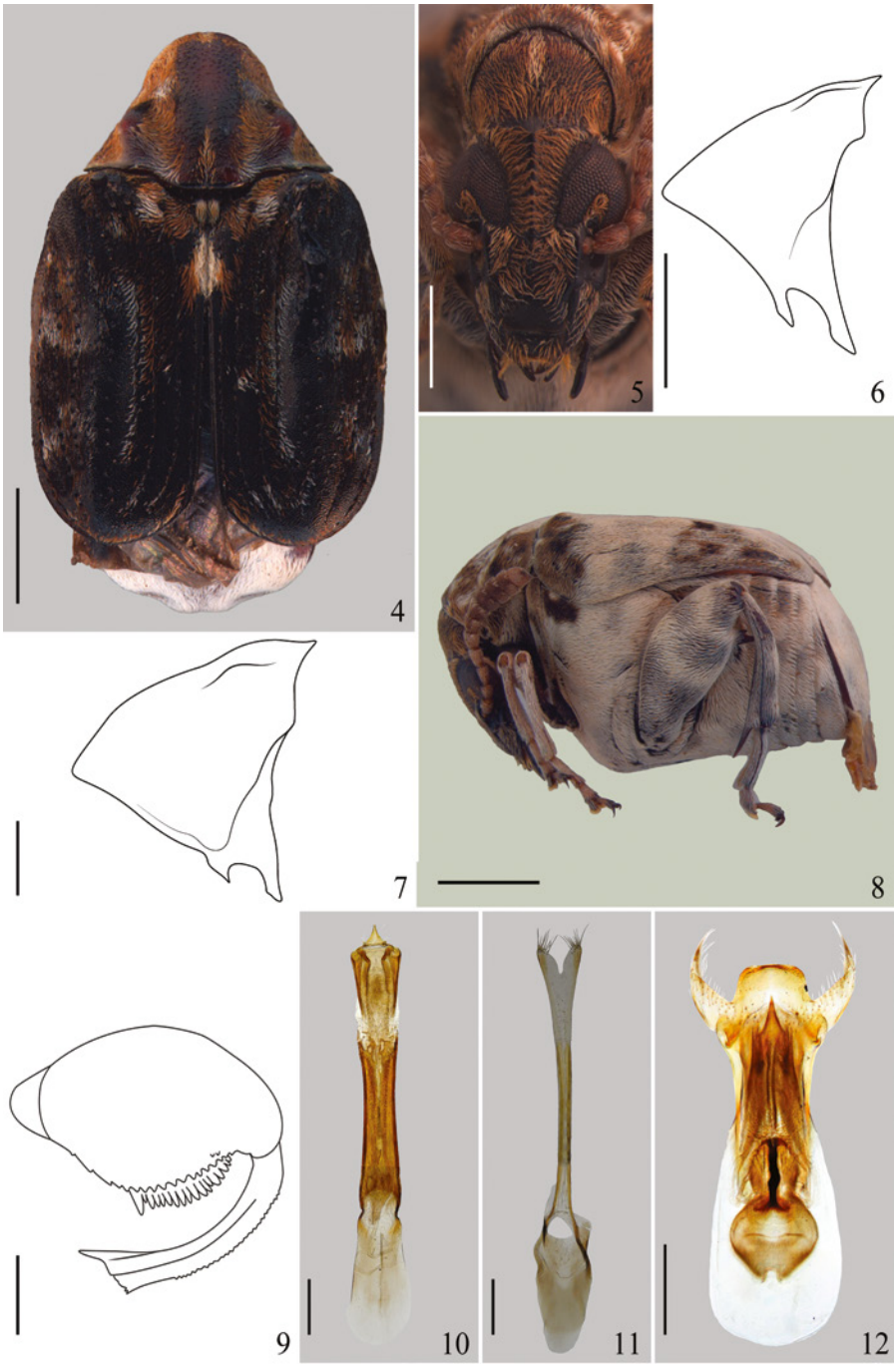

Figs. 4–12. Dorsal habitus, *Ctenocolum acapulcensis*; 5. Head, frontal view, *Caryedes quadridens*; 6–7. Pronotum, lateral view: 6. *Ctenocolum podagricus*; 7. *C. acapulcensis*; 8. Lateral view, *C. quadridens*; 9. Posterior leg, external view, *C. janzeni*; 10–12. Male genitalia: 10–11. *C. quadridens*: 10. Median lobe; 11. Tegmen; 12. Median lobe, *Pygiopachymerus lineola*. Scales. 3, 7–8: 1mm; 5–6, 9: 0.5mm; 10–12: 0.25.

C. podagricus (on *Piscidia* but also on *Schnella* Raddi, a member of the Cercideae tribe). Besides these expansions, one species (*C. salvini*) shifted on a plant genus (*Dalbergia*) belonging to a distantly related tribe, the Dalbergieae. As underlined in Wink (2013) both Dalbergieae and Millettieae have independently evolved the capacity to produce rotenone. Hence we can hypothesize that the shift on *Dalbergia* has been facilitated by pre-existing adaptions to rotenoids toxic compounds in *Ctenocolum* beetles. This finding provides another line of evidence supporting the potential role of chemical specialization as a major evolutionary driver in the evolution of host-use in seed-beetles (see also Kergoat et al. 2005b; Kergoat et al. 2007a).

Biogeographic analyses indicate that the genus *Ctenocolum* originated and diversified in South America, in the Brazilian subregion. The diversification of the group in this subregion matches those of their main host plants (*Lonchocarpus* and *Piscidia*), which are also more diverse in the Brazilian subregion (da Silva 2010; da Silva & Tozzi 2012). From there, two species (*C. aquilus* and *C. milelo*) colonized the Chacoan subregion. Another species, *C. pygospilotus*, also colonized the Antillean subregion. Only one species, *C. podagricus*, is found in the Nearctic region. This species has a range that encompasses the Antillean and Chacoan subregions, the Mexican transition zone and the Nearctic region. Because *C. podagricus* is also the species with the broadest host plant range a parallel can be drawn with patterns evidenced in Nymphalinae butterflies, where 'species feeding on a large number of host plants tend to have larger geographic ranges than species feeding on fewer plants' (Slove & Janz 2011).

Taxonomy

Group *tuberculatum*

The group *tuberculatum* was recovered as monophyletic in the parsimony phylogenetic analysis (Figure 1A). The new species *Ctenocolum inmaculatus* Manfio & Ribeiro-Costa **sp. nov.**, described below, appears as sister to *C. tuberculatum.* A complete list of characters to diagnose this group can be found in Albuquerque et al. (2014; p. 35).

Ctenocolum inmaculatus Manfio & Ribeiro-Costa **sp. nov.** (Figures 12–19)

ZooBank: http://zoobank.org/0326E29C-547F-473E-B1EE-52E006A3BF75

Material Examined

Type material. Holotype, deposited in USNM, male: (1) "VENEZUELA/Guar., 12KmS./Calabozo/II-6-12-1969/P. & P. Spangler" (2) "Est. Biologica/Los Llanos/ Black Light" (3) "HOLOTYPE/*Ctenocolum inmaculatus*/Manfio & Ribeiro-Costa".

Diagnosis

Ctenocolum inmaculatus Manfio & Ribeiro-Costa **sp. nov.** differs from *C. tuberculatum* by the morphology of the sclerite, smooth, subretangulate with sinuous stems oriented

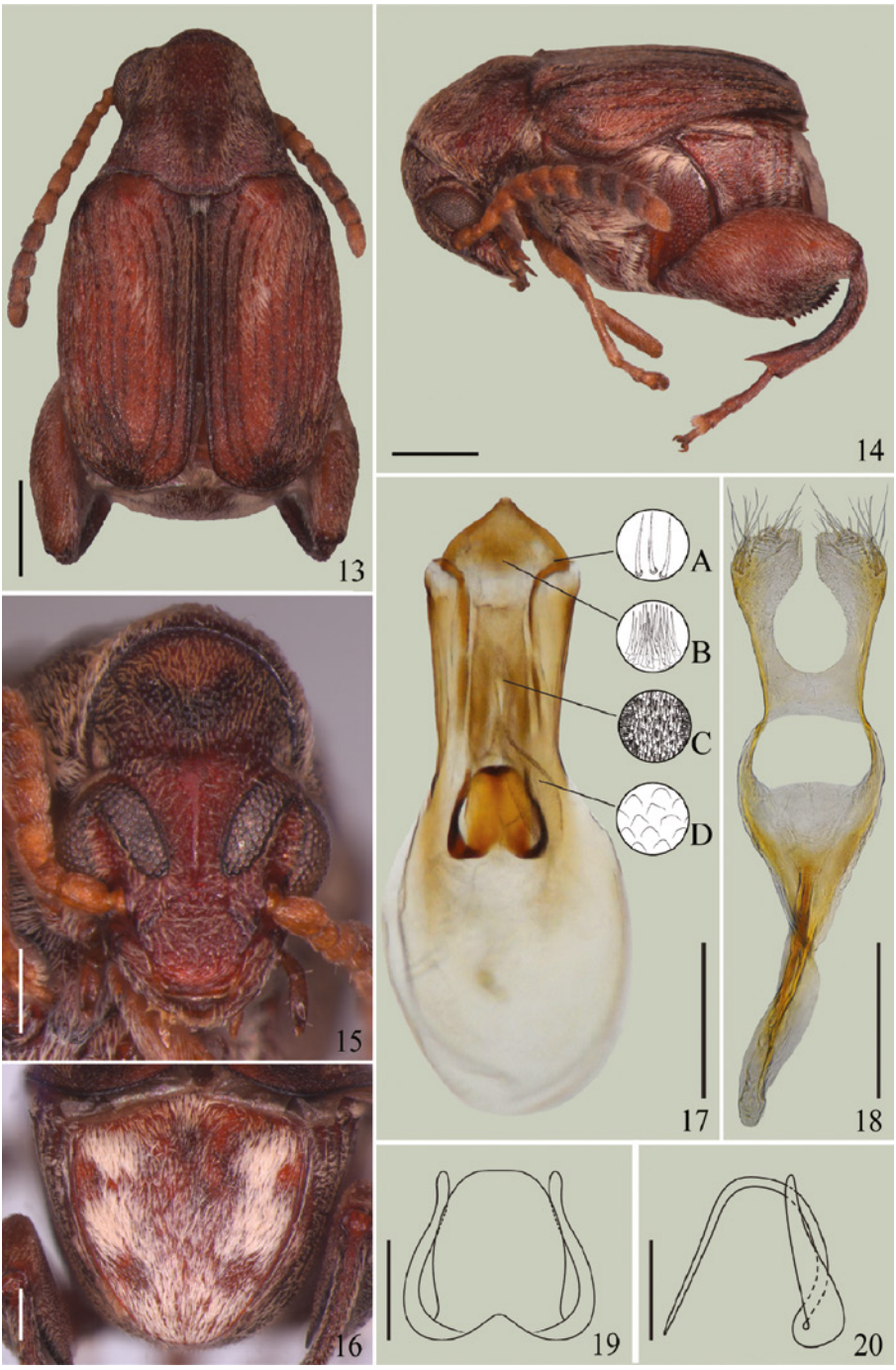

Figs. 13–20. *Ctenocolum inmaculatus* **sp. nov.**: 13. Dorsal habitus; 14. Lateral habitus; 15. Head, frontal view; 16. Male pygidium; 17–20. Male genitalia: 17. Median lobe; 18. Tegmen; 19–20. Submedian smooth sclerite: 19. Ventral view; 20. Lateral view. Scales: 13–14. 0.5 mm; 15–16. 0.2 mm; 17–18. 0.25 mm; 19–20. 0.1 mm.

forward, as long as the central region (Figures 17, 19–20); from the other species of the group *tuberculatum* it differs by the dorsum not variegated and the integument on pronotum reddish brown and on elytra brown with dark brown areas (Figure 13).

Description

Holotype male. BL: 2.65 mm; BW: 1.71 mm.

Integument. *Pronotum* (Figure 13): reddish brown; posterior region of median gibbosity with two short dark brown horizontal strip. *Elytron* (Figure 13): brown with dark brown areas at humerus, internal region and apex (Figure 13). *Antenna* (Figure 13): pale brown, antennomeres 8–10 dark brown. *Pygidium* (Figure 16): brown with dark brown spots. *Ventral region* (Figure 14): mainly reddish brown and dark brown; front and middle legs pale brown; hind leg brown and reddish brown.

Pubescence. *Pronotum* (Figure 13): with almost uniform, white and pale brow, except dark brown pubescence in the short dark brown horizontal strips at posterior region of median gibbosity. *Elytron* (Figure 13): mainly pale brow, denser pubescence in an inverted triangular area at basal half; white pubescence mainly conspicuous at base, in an oblique strip between the striae 2–3 and at median region in a conspicuous short strip at interstriae 4 and 5. *Pygidium* (Figure 16): yellowish gray, dense except on four lateral and median areas. *Ventral region* (Figure 14): mainly white.

Head (Figure 15). Ocular sinus 0.44 mm; ocular index 5.68; length of eyes in frontal view behind sinus 0.19 mm. Antenna serrate from antennomeres 4–10 (Figure 14).

Prothorax. Pronotum with median gibbosity moderately elevated, divided by longitudinal and by transversal sulcus; lateral gibbosity moderately elevated; basal lobe without median depression and slightly emarginated (Figures 13, 14).

Mesothorax and metathorax. Elytron, striae with elongated and slightly impressed punctures (Figure 13); small and teeth at base of striae 3 and 4, parallel to each other; tooth of stria 4 closer to base of tooth of stria 3 than to anterior margin of elytra; stria 6 conspicuously impressed (Figure 13). Hind femur (Figure 14) on external ventral margin with toothed carina; without denticles above external ventral margin; pecten with 12 teeth. Hind tibia (Figure 14) straight beside mucro, coronal tooth absent; inconspicuous lateral coronal denticles.

Abdomen. Pygidium (Figure 16) as long as wide, subtriangulate, with moderately impressed punctures.

Male genitalia. *Median lobe* (Figure 17): ventral valve about 1.7 x wider than long, lateral margins convergent on apical region, rounded apical border, basal margin emarginated, about half length of valve, lateral base with tuft of setae (Figure 17A). Internal sac, apical region with group of spicules medially (Figure 17B), hinge sclerite with inverted L-shaped, long, extending to median region; subapical to median region with long rectangular structure; median to submedian region with dense spicules laterally (Figure 17C); submedian region with smooth sclerite, subretangulate with sinuous stems oriented backward, as long as the central region (Figures 17, 19–20), sparse scales (Figure 17D). *Tegmen* (Figure 18): lateral lobes separated by emargination

about 0.8 times the length of lateral lobes; apex internally expanded, about 3 times the smaller width on median region, setae on outer surface moderately elongated, without obtuse or acute tooth, without membranous projection; internal margin near end of emargination rounded, forming a "U"; base with a dorsal process (see Figure 27 of *C. biolleyi*); tegminal strut with dorsal and ventral keel.

Female

Unknown.

Distribution

Venezuela (Guarico).

Known host plant(s)

Unknown.

Etymology

The specific epithet 'immaculatus' of *C. inmaculatus* is Latin for immaculate in allusion to the integument and pubescence pattern on dorsum, lacking stripes or patches.

Group *podagricus*

Phylogenetic analyses showed that *Ctenocolum biolleyi*, *C. nigronotus* Manfio & Ribeiro-Costa **sp. nov.** and *C. pallidus* Manfio & Ribeiro-Costa **sp. nov.** belong to the group *podagricus* (Figure 1A). A complete list of diagnostic characters for this group can be found in Albuquerque et al. (2014; p. 17).

***Ctenocolum biolleyi* Kingsolver & Whitehead, 1974** (Figures 21–27, 42)

Material Examined

USNM. 7 males, 5 females: (1) "COSTA RICA/Punt. Prov./Cuajiniquil/Nicoya Penins." (2) "II-1983, in/Lonchocarpus sp./Lupo Espinosa leg.". 1 male: idem (1) and (2) labels; (3) "Ctenocolum/biolleyi/K+W/J. Kingsolver

Diagnosis and a complete list of literature

See Albuquerque et al. (2014; p. 24).

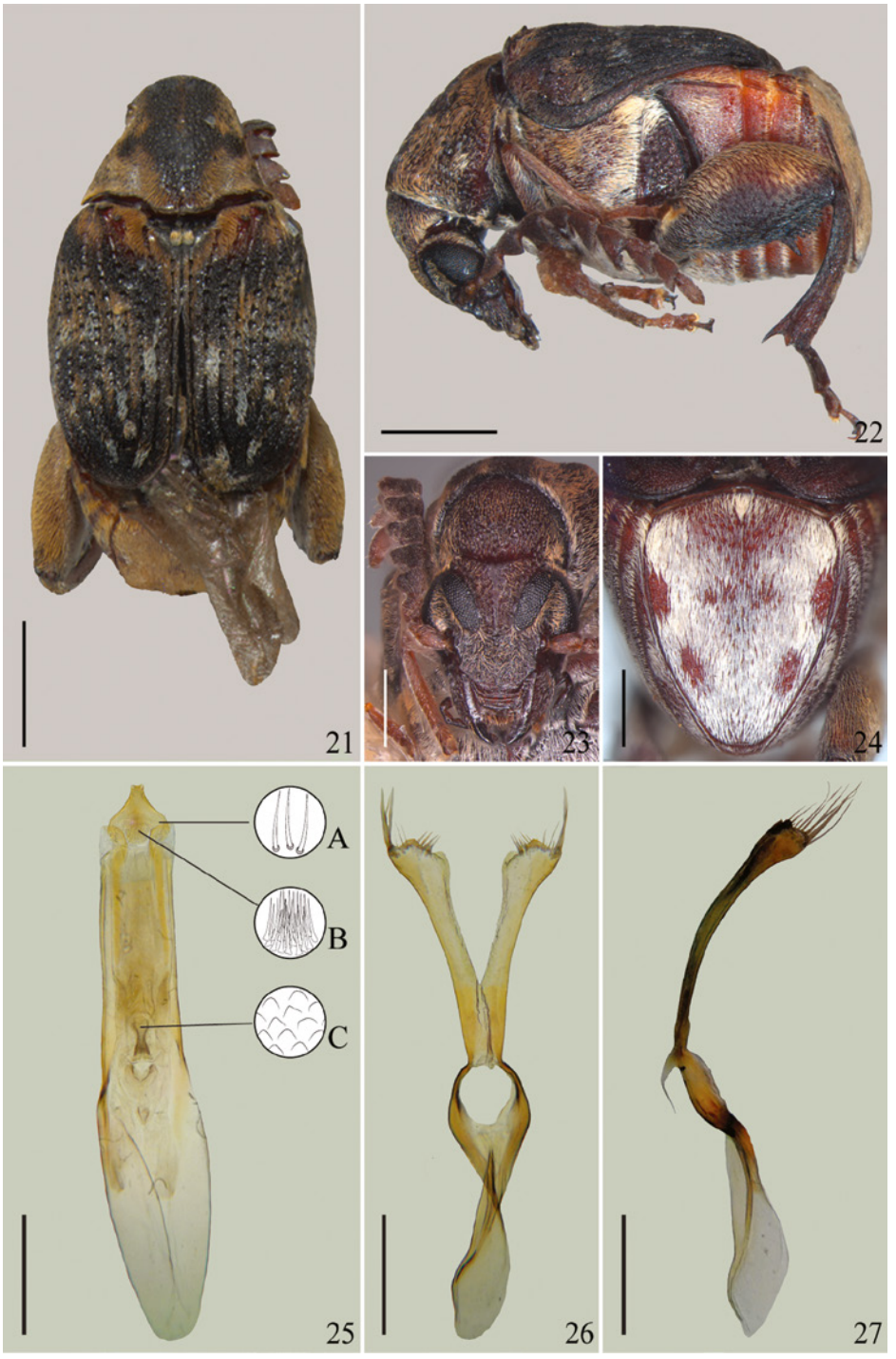

Figs. 21–27. *Ctenocolum biolleyi*: 21. Dorsal habitus; 22. Lateral habitus; 23. Head, frontal view; 24. Male pygidium; 25–27. Male genitalia: 25. Median lobe; 26–27. Tegmen: 26. Ventral view; 27. Lateral view. Scales: 21–22. 1 mm; 23–24. 0.5 mm; 25–27. 0.25 mm.

Description

Male. BL: 4.2–4.4 mm; BW: 2.8–2.9 mm.

Integument. *Antenna*: mostly black or dark brown (Figure 22).

Pubescence. *Pronotum* (Figure 21): oval area wider than in female, almost glabrous, divided by a very narrow longitudinal strip, apparently absent transversal strip. *Elytron* (Figure 21): variegated pattern less conspicuous than in female, mainly white setae forming some short vertical strips; denser brown pubescence near scutellum. *Pygidium* (Figure 22): white or pale brown, dense, except the four lateral small areas and a larger area from basal to median region. *Ventral region* (Figure 22): pale brown and white.

Head. *Antennae* (Figure 22)*:* serrate from antennomere 4 in male and from antennomere 5 in female; generally longer in male than in female, reaching the middle of elytra when the head is next to the body.

Male genitalia. *Median lobe* (Figure 25): ventral valve wider than long, lateral margins subparallels on apical region, basal margin emarginated, lateral base with tuft of setae (Figure 25A). Internal sac, apical region with group of spicules medially (Figure 25B), hinge sclerite similar to stick, long, extending to median region; subapical region with small and very thin dense spicules directed towards apex; median region with lateral stripes of small and very thin spicules directed towards middle and median spicules towards apex; submedian region with squamous hourglass-shaped structure and arcuate structure bellow (Figures 25, 25C); basal region bilobate, small denticles at lobes. *Tegmen* (Figures 26–27): lateral lobes separated by emargination about 0.65 times the length of lateral lobes; apex externally expanded, about 2.5 times the smaller width on median region, divergent external margins, long setae on outer surface, median blind obtuse tooth, without membranous projection; internal margin near end of emargination straight, forming a "V"; base with a dorsal process (Figure 27); tegminal strut with dorsal and ventral keel.

Female

Sternite VIII (Figure 42): longer than wide (from apex to spiculum ventrale insertion).

Distribution

Costa Rica (Puntarenas Province, San Jose).

Known host plant(s)

Lonchocarpus eriocarinalis (Fabaceae, Papilionoideae, Millettieae).

Ctenocolum nigronotus Manfio & Ribeiro-Costa sp. nov. (Figures 28–34)

ZooBank: http://zoobank.org/5A76DED6-03E6-4B40-B1C1-57ADB79A9FF9

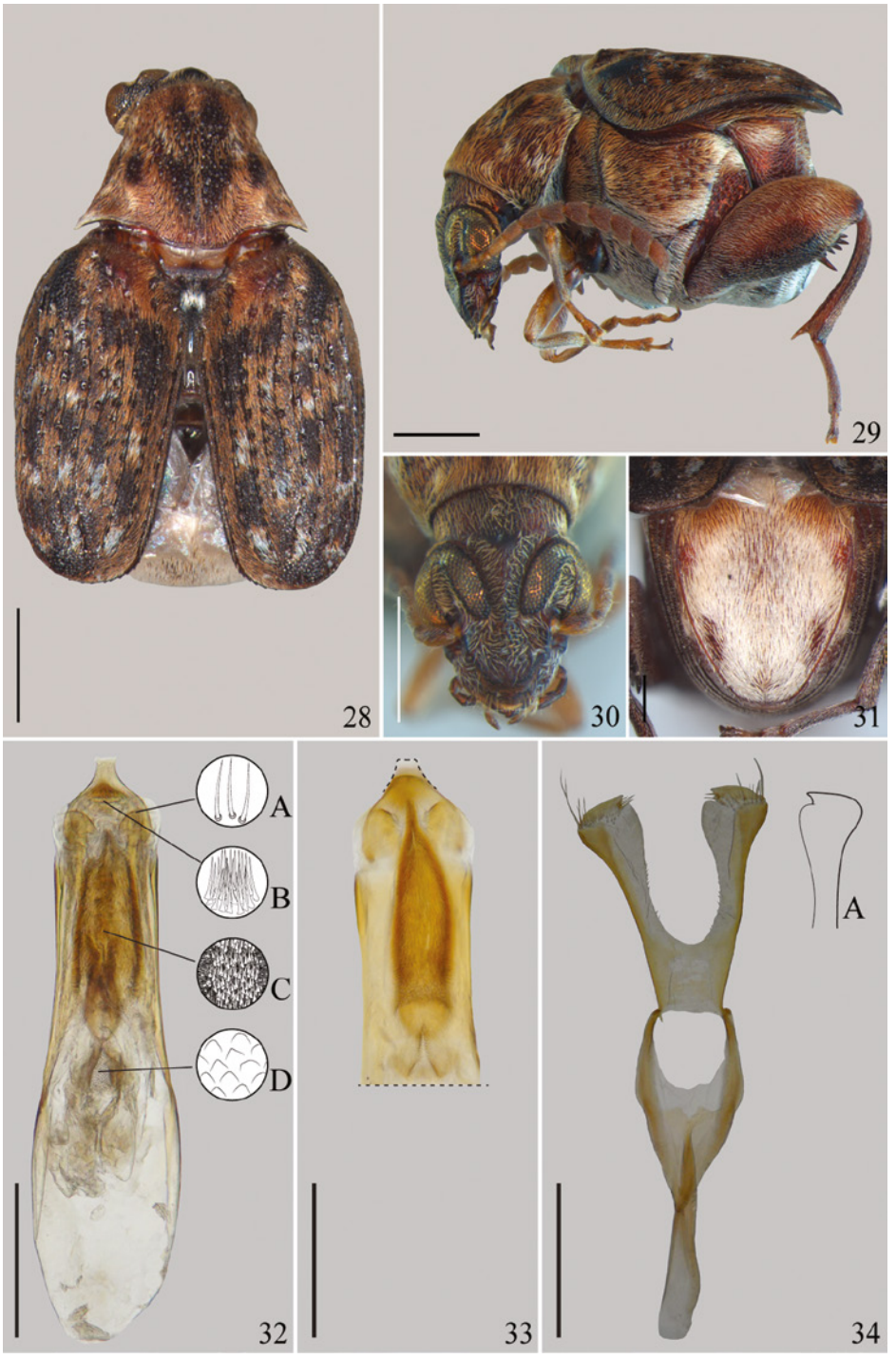

Figs. 28–34. *Ctenocolum nigronotus* **sp. nov.**: 28. Dorsal habitus; 29. Lateral habitus; 30. Head, frontal view; 31. Male pygidium; 32–34. Male genitalia: 32. Median lobe; 33. Median lobe, apical half; 34. Tegmen. Scales: 28–30. 0.5 mm; 31. 0.2 mm; 32–34. 0.25 mm.

Material Examined

Type material. Holotype, deposited in USNM, male: (1) "Mayaguez/PR #1770" (2) "Piscidia erythrina x,12'36/RHMoore thru/L. C. McAlister" (3)"HOLOTYPE/*Ctenocolum nigronotus*/Manfio & Ribeiro-Costa". Paratypes. 7 males deposited in USNM: (1) and (2) same labels of the Holotype (3) "PARATYPE/*Ctenocolum nigronotus*/Manfio & Ribeiro-Costa".

Diagnosis

Ctenocolum nigronotus Manfio & Ribeiro-Costa **sp. nov.** differs from the other species of the group *podagricus* mainly by the median lobe of median genitalia with two spiculated tubular structures partially overlapped (Figure 32–33). Besides, this species is also different in the pubescence pattern on elytra, with golden, brown and black setae mainly forming elongated, intercalated strips and white pubescence forming short strips and patches and course and rounded punctures (Figure 28).

Description

Holotype male. BL: 2.64 mm; BW: 1.81 mm.

Integument. *Pronotum* (Figure 28): black and reddish brown. *Elytron* (Figure 28): black. *Antenna* (Figure 29): mainly brown, first three antennomeres yellow ochre and dark brown. *Pygidium* (Figure 31): brown and reddish brown. *Ventral region* (Figure 29): dark brown, reddish brown and brown; last abdominal ventrite pale brown; front and middle legs mainly yellow ochre; hind femur bicolor, brown dorsal half and dark brow ventral half.

Pubescence. *Pronotum* (Figure 28): predominantly golden brown with white patches; sparse setae exposing the integument forming an oval, wide area from anterior to posterior region divided by transversal and longitudinal strip of denser setae and in one small area on each lateral gibbosity. *Elytron* (Figure 28): golden, brown and black pubescence mainly forming elongated intercalated strips; white pubescence forming short strips and patches. *Pygidium* (Figure 31): dense white, golden brown at base; four glabrous lateral areas. *Ventral region* (Figure 29): predominantly white, golden brown mainly at mesepisternum, mesepimerum and metepisternum.

Head (Figure 30). Ocular sinus 0.48 mm; ocular index 5.14; length of eyes in frontal view behind sinus 0.18 mm. Antenna serrate from antennomeres 4–10 (Figure 29).

Prothorax. Pronotum with median gibbosity moderately elevated, divided by longitudinal and transversal sulcus; lateral gibbosity moderately elevated; basal lobe without median depression and with emarginated border (Figures 28–29).

Mesothorax and metathorax. Elytra, striae with strongly impressed and rounded punctures (Figure 28); large teeth at base of striae 3 and 4, oblique to each other; tooth of stria 4 closer to base of tooth of stria 3 than to anterior margin of elytra; stria 6 conspicuously impressed (Figure 28). Hind femur (Figure 29) on external ventral margin

with toothed carina; without denticles above external ventral margin; pecten with 7 teeth. Hind tibia (Figure 29) emarginated beside mucro; small coronal tooth; lateral coronal denticles present.

Abdomen. Pygidium longer than wide, oval (Figure 31).

Male genitalia. *Median lobe* (Figures 32–33): ventral valve about 1.15 x wider than long, lateral margins subparallel on apical region, apical border straight, basal margin emarginated, about 1/3 length of valve lateral base with tuft of setae (Figure 32A). Internal sac, apical region with group of spicules medially (Figure 32B), hinge sclerite short, extending only subapical region; apical to subapical region with a large tubular structure covered by long and dense spicules (Figure 32C), acute apex, opened dorsally, partially overlapping the median structure; subapical to median region with long structure covered by long and dense spicules (Figure 32C); submedian region squamous sphere-shape structure (Figures 32, 32D); basal region bilobate. *Tegmen* (Figure 34): lateral lobes separated by emargination about 0.7 times the length of lateral lobes; apex internally and externally expanded, about 2.7 times the smaller width on median region, setae on outer surface moderately elongated, inner acute tooth directed towards middle (Figure 34A), without membranous projection; internal margin near end of emargination straight, forming a slight "V"; base with a dorsal process (see Figure 27 of *C. biolleyi*); tegminal strut with dorsal and ventral keel.

Variability

BL: 2.24–2.62 mm; BW: 1.5–1.79 mm.

Integument. Elytra black and reddish brown. Hind femur, reddish brown dorsal half.

Pubescence. Pygidium median area slightly less dense areas.

Head. Ocular sinus 0.41–0.51 mm; ocular index 4.96–5.7; length of eyes in frontal view behind sinus 0.17–0.22 mm.

Prothorax. Pronotum, basal lobe with median depression and slightly emarginated border. Hind femur, pecten with 6 or 8 teeth. Hind tibia, larger small coronal tooth.

Female

Unknown.

Distribution

Puerto Rico (Mayaguez).

Known host plant(s)

Piscidia piscipula (L.) Sarg. (= *Piscidia erythrina* L.) (Fabaceae, Papilionoideae, Millettieae).

Etymology

The specific name '*nigronotus*' denotes the color of the integument. In Greek 'nigra' means 'black' and 'notus' means 'back'; refers to the blackish integument at the dorsal side of this new seed beetle.

Ctenocolum pallidus Manfio & Ribeiro-Costa sp. nov. (Figures 35–41, 43)

ZooBank: http://zoobank.org/7557E967-229B-461D-AEAD-F2250D18D4B6

Material Examined

Type material. Holotype, deposited in USNM, male: (1) "in/Muellera seed/Br.Guiana/ Oct. 1, '34 at/Wash. DC/H Y Gouldman/BPQ 020678" (2) "HOLOTYPE/*Ctenocolum pallidus*/Manfio & Ribeiro-Costa". Paratypes. 8 deposited in USNM, 2 males: (1) same label of the Holotype (2) "PARATYPE/*Ctenocolum pallidus*/Manfio & Ribeiro-Costa"; 3 males and 3 females: (1) "Muellera seed/Br. Guiana/X-1-34/BPQ 030678" (2) same label of Paratype.

Diagnosis

Ctenocolum pallidus Manfio & Ribeiro-Costa **sp. nov.** differs from the other species of the group *podagricus* because of the color on dorsum, the integument is slightly variegated mainly pale brown, brown and yellow ochre and the pubescence predominantly yellowish gray, white and pale brown (Figure 35).

Description

Holotype male. BL: 2.86 mm; BW: 1.96 mm.

Integument. *Pronotum* (Figure 35): brown. *Elytron* (Figure 35): slightly variegated, pale brown to brown, yellow ochre in the apical margins; except the reddish brown humeral region; subbasal region, interstria 3, median region, interstria 5–10; apical small macula between the striae 3–9. *Antenna* (Figure 36): yellowish ochre, apex of the antennomeres slightly yellow ochre. *Pygidium* (Figure 38): brown and pale brown. *Ventral region* (Figure 36): pale brown, brown and dark brown except for front and middle legs yellow ochre.

Pubescence. *Pronotum* (Figure 35): uniform, predominantly yellowish gray with two vertical pale brown strips. *Elytron* (Figure 35): interstriae 1–2 yellowish gray, rest of the elytra variegated white, yellowish gray, pale brown and black. *Pygidium* (Figure 35; apparently damaged pubescence): yellowish gray, denser at latero basal areas and apical region. *Ventral region* (Figure 36): mainly yellowish gray.

Head (Figure 37). Ocular sinus 0.46 mm; ocular index 7.6; length of eyes in frontal view behind sinus 0.3 mm. Antenna serrate from antennomeres 4–10 (Figure 35).

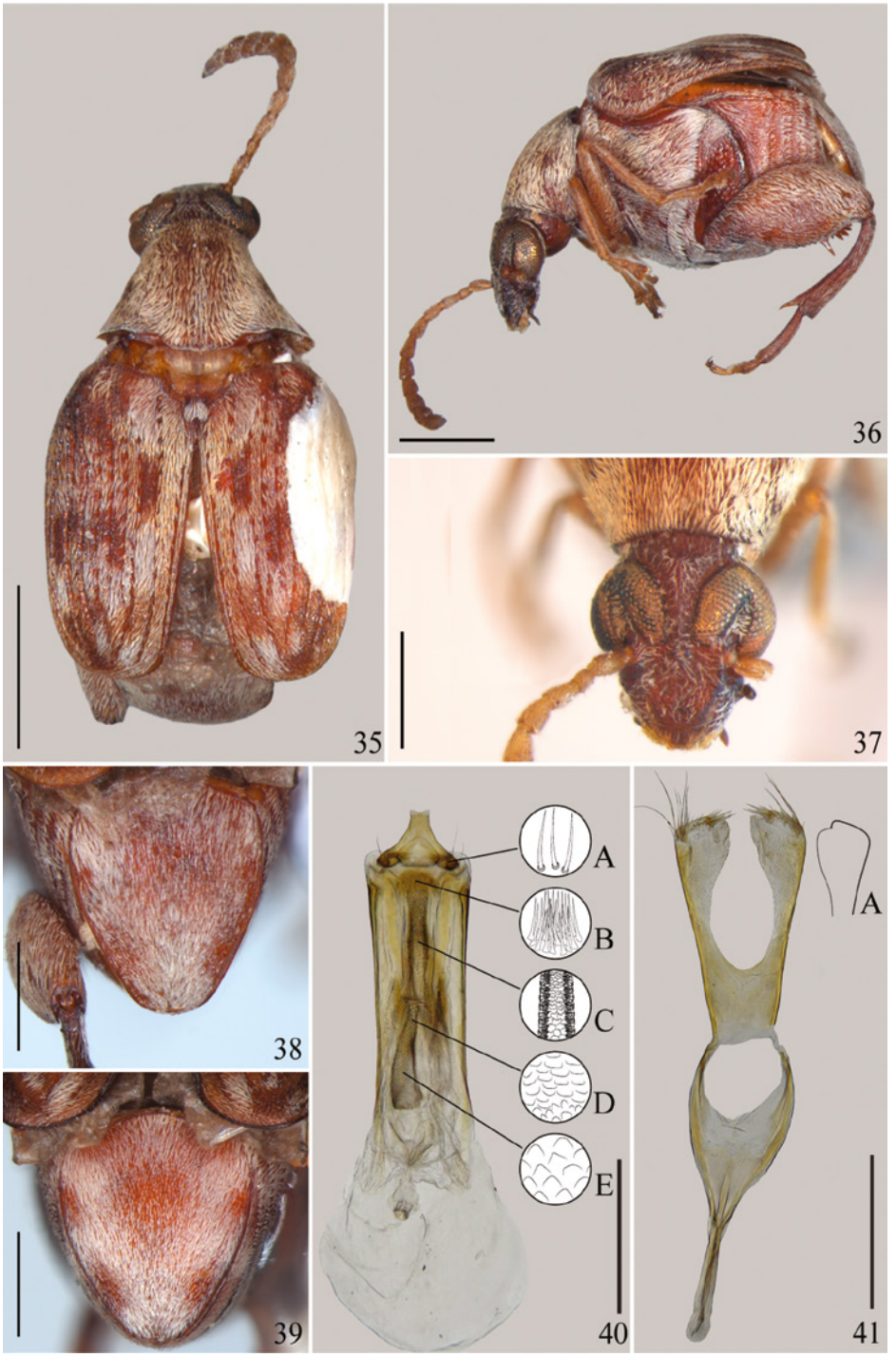

Figs. 35–41. *Ctenocolum pallidus* **sp. nov.**: 35. Dorsal habitus; 36. Lateral habitus; 37. Head, frontal view; 38–39. Pygidium: 38. Male; 39. Female; 40–41. Male genitalia: 40. Median lobe; 41. Tegmen. Scales: 35–36. 1 mm; 37–39. 0.5 mm; 40–41. 0,25 mm.

Prothorax. Pronotum with median gibbosity slightly elevated, not divided by longitudinal and transversal sulcus; lateral gibbosity slightly elevated; basal lobe with a median depression and with a strong emarginated border (Figures 35–36).

Mesothorax and metathorax. Elytra, striae with moderately impressed and slightly elongated punctures (Figure 35); small teeth at base of striae 3 and 4, oblique to each other; tooth of stria 4 closer to base of tooth of stria 3 than to anterior margin of elytra; stria 6 conspicuously impressed (Figure 35). Hind femur (Figure 36) on external ventral margin with toothed carina; without denticles above external ventral margin; pecten with 7 teeth. Hind tibia (Figure 36) emarginated beside mucro; small coronal tooth; lateral coronal denticles present.

Abdomen. Pygidium longer than wide, oval, moderately impressed punctures (Figure 38).

Male genitalia. *Median lobe* (Figure 40): ventral valve about 1.5x wider than long, lateral margins subparallel on apical region, basal margin strongly emarginated, more than half length of valve, lateral base with tuft of setae (Figure 40A). Internal sac, apical region with group of spicules medially (Figure 40B), hinge sclerite similar to stick, long, extending to subapical region; apical to subapical region with median, long, tubular squamous-spiculated structure, opened dorsally, partially overlapping the median structure, irregular scales, short spicules and lateral dense small and thin spicules (Figure 40C); median to submedian region with median, long, tubular squamous structure, rounded scales (Figures 40D, 40E); apical region bilobate. *Tegmen* (Figure 41): lateral lobes separated by emargination about 0.65 times the length of lateral lobes; apex internally expanded, about 3 times the smaller width on median region, long setae on outer surface, inner blind obtuse tooth (Figure 41A), without membranous projection; internal margin near end of emargination curved, forming a "U"; base with a dorsal process (see Figure 27 of *C. biolleyi*); tegminal strut with dorsal and ventral keel.

Variability

Body. Length: 1.57–2.17 mm; width: 2.18–3.27 mm.

Integument. *Pronotum*: reddish brown or reddish brown and dark brown. *Elytron*: more conspicuously variegated with dark brown integument at humeral region (dark region reaching or not the subbasal region), subbasal strip in the interstria 3, median strips in the interstriae 5–10 and apical small macula. *Antenna*: yellowish in the first antennomeres subtly becoming yellowish ochre towards the apex. *Ventral region*: brown, reddish brown and dark brown.

Pubescence. *Pronotum*: black in a large central macula and lateral small maculae. *Elytron*: interstriae 1–2 pale brown, rest of the elytra variegated white, pale brown and black. *Pygidium*: four lateral small areas and a large median area exposing the integument.

Head. Ocular sinus 0.34–0.6 mm; ocular index 5.5–7.75; length of eyes in frontal view behind sinus 0.28–0.36 mm (n = 7).

Mesothorax and metathorax. Hind femur, pecten with 5–6 teeth.

Female

Sternite VIII (Figure 43): wider than wide (from apex to spiculum ventrale insertion).

Distribution

Republic of Guyana (previously British Guyana).

Known host plant(s)

Muellera sp. (Fabaceae, Papilionoideae, Millettieae). This is the first species of *Ctenocolum* recorded on *Muellera*.

Etymology

Ctenocolum pallidus was named because of the light color on dorsum, mainly pale brown, brown and yellow ochre.

Updated key to *Ctenocolum species*

To accommodate the three species described here, the key to the *Ctenocolum* species proposed by Albuquerque et al. (2014, p. 16) is modified as follows:

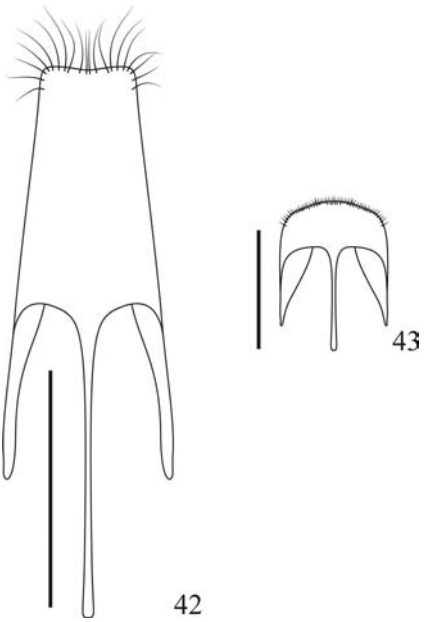

Figs. 42–43. Sternite VIII: 42. *Ctenocolum biolleyi*; 43. *C. pallidus* **sp. nov.** Scales: 42. 1 mm; 43. 0.5 mm.

1. Hind femur, pecten regular from second tooth towards distal region (Figure 14; and see Albuquerque et al. 2014: p. 15, Figures 75–76; p. 16, Figures 77–78); hind tibia on outer surface with row of denticles (Figure 9; and see Albuquerque et al. 2014: p. 4, Figure 4; p. 15, Figures 75–76; p. 16, Figures 77–78), apex lightly or moderately emarginated beside mucro (Figures 9, 14; and see Albuquerque et al. 2014: p. 15, Figures 75–76; p. 16, Figures 77–78) (Group *tuberculatum*). 2

2'. Hind femur, pecten increasing in size until middle and decreasing from second tooth gradually towards distal region with second tooth of pecten gradually increasing in size until middle and decreasing towards apex (Figures 22, 29, 36; and see Albuquerque et al. 2014: p. 14, Figures 66–71; p. 15, Figures 72–74); hind tibia on outer surface without row of denticles, apex strongly emarginated beside mucro (Figure 22; and see Albuquerque et al. 2014: p. 14, Figures 66–71; p. 15, Figures 72–74) (Group *podagricus*). 5A

2 (1). Antennomeres 8–10 darker than the others (Figure 14; and see Albuquerque et al. 2014: p. 6, Figures 18–19, 21; p. 13, Figures 63, 65); internal sac at apex laterally with short tuft of setae (see Albuquerque et al. 2014: p. 19, Figure 90); tegmen, lateral lobe at apex without membranous projection (Figure 18; and see Albuquerque et al. 2014: p. 20, Figure 99; p. 21, Figure 100, 102). 3

2'. Antennomeres 8–10 the same color as the others (see Albuquerque et al. 2014: p. 6, Figure 20; p. 13, Figure 64); internal sac at apex laterally with long tuft of setae (see Albuquerque et al. 2014: p. 4, Figure 5; p. 19, Figure 89); tegmen at apex of lateral lobe with membranous projection (see Albuquerque et al. 2014: p. 4, Figure 7) ..... *C. salvini* (Sharp, 1885)

3 (2). Hind femur on external ventral margin without toothed carina (see Albuquerque et al. 2014: p. 15, Figure 75). .....*C. acapulcensis* Kingsolver & Whitehead, 1974

3'. Hind femur on external ventral margin with toothed carina (see Albuquerque et al. 2014: p. 15, Figure 76; p. 16, Figure 78). 4

4(3'). Hind femur with denticles on the external ventral margin (see Albuquerque et al. 2014: p. 15, Figure 76); Male pygidium longer than wide, oval (Figure 9)..... *C. janzeni* Kingsolver & Whitehead, 1974

4'. Hind femur without denticles on external ventral margin (see Albuquerque et al. 2014: p. 16, Figure 78); Pygidium as long as wide, subtriangulate (Figure 16). 4A

4A(4'). Elytra strongly variegated; denser pubescence, brown, yellowish gray, black and white, sometimes without black setae; integument black or black and reddish brown (see Albuquerque et al. 2014: p. 6, Figure 21). .... *C. tuberculatum* (Motschulsky, 1874)

4A'. Elytra not variegated; mostly with sparse pale brown pubescence, exposing the brown integument with dark brown areas at humerus, internal region and apex (Figure 13). ..... *C. inmaculatus* Manfio & Ribeiro-Costa **sp. nov.**

5A(2'). Dorsum, integument predominantly brown (Figure 35) .... *C. pallidus* Manfio & Ribeiro-Costa **sp. nov.**

5A'. Dorsum, integument never predominantly brown, mostly dark brown to black (Figure 28). 5

5(5A'). Dorsum mostly with yellowish gray setae, forming a "C" pattern on each elytron (see Albuquerque et al. 2014: p. 5, Figure 10); pronotum with sparse setae that exposes the integument and forms a rounded area on anterior region (see Albuquerque et al. 2014: p. 5, Figure 10). ..... *C. colburni* Kingsolver & Whitehead, 1974

5'. Dorsum never mostly yellowish gray; when mostly yellow gray, not forming a conspicuous pattern on each elytron like a "C" (see Albuquerque et al. 2014: p. 5, Figures 8–9, 11–16; p. 6, Figure 17); pronotum with sparse pubescence exposing the integument forming an oval, wide area from anterior to posterior region, divided or not by transversal and longitudinal strip of denser setae (Figure 28; and see Albuquerque et al. 2014: p. 5, Figures 8–9, 11–16; p. 6, Figure 17). 6

6 (5'). Elytral striae with deeply impressed punctures (Figure 28; and see Albuquerque et al. 2014: p. 5, Figures 15–16). 6A

6'. Elytral striae with moderately impressed punctures (see Albuquerque et al. 2014: p. 5, Figures 8-9, 11–14; p. 6, Figure 17). 8

6A (6). Elytra strongly variegate, with golden brown and black pubescence mainly forming elongated intercalated strips; white pubescence forming short strips and patches (Figure 28). .... *C. nigronotus* Manfio & Ribeiro-Costa **sp. nov**.

6A'. Elytra slightly variegated, yellowish gray and white (see Albuquerque et al. 2014: p. 5, Figures 15–16). 7

Couplets 7–12 without change.

New host plant and distribution records
Ctenocolum podagricus (Fabricius, 1801)

New host plant record: *Lonchocarpus sericeus* (Poir.)Kunth *ex* DC. Material examined: 1, (1) "in Seed Lonch-/ocarpus seri-/ceus Venez./7.27'H2 SF 18130" (2) "Caryedes/sp/HSB'H2".

New distribution record: Dominican Republic (Dajabon Province).

Material examined: 1, (1) "DOMINICAN REPUBLIC:/Dajabon Province/13km S. Loma de Cabrera/ca. 400m, 20–22 May 1973/Don & Mignon Davis" (USNM).

Acknowledgments

We are grateful to the editor, Hojun Song, and to one anonymous reviewer for their constructive and insightful comments. We thank Alexander Konstantinov and Elisabeth Roberts, United States National Museum, Smithsonian Institution, that kindly received the two first authors in the USNM and for the loan of specimens that

enable this study; the Coordenação de Aperfeiçoamento de Pessoal de Nível Superior (CAPES) for the scholarship for the first author and the Conselho Nacional de Desenvolvimento Científico e Tecnológico (CNPq) for the scholarships for the second and fourth authors; Alexandre Dehne Garcia for his help on the CBGP HPC computational platform. This is the contribution number 1937 of the Departamento de Zoologia, Universidade Federal do Paraná, Curitiba, Brazil.

References

Albuquerque, F.P., Manfio, D. & Ribeiro-Costa, C.S. (2014) A contribution to the knowledge of New World Bruchinae (Coleoptera, Chrysomelidae): taxonomic revision of *Ctenocolum* Kingsolver & Whitehead, with description of five new species. *Zootaxa* **3838**: 1–45.

Alvarez, N., Romero-Napoles, J., Anton, K.W., Benrey, B. & Hossaert-McKey, M. (2006) Phylogenetic relationships in the Neotropical bruchid genus *Acanthoscelides* (Bruchinae, Bruchidae, Coleoptera). *Journal of Zoological Systematics and Evolutionary Research* **44**: 63–74.

Bisby, F.A., Buckingham, J. & Harborne, J.B. (1994) *Phytochemical Dictionary of the Fabaceae. vol. 1. Plants and their Constituents.* Chapman and Hall, London: 357 pp.

Borowiec, L. (1987) The genera of seed beetles (Coleoptera, Bruchidae). *Polskie Pismo Entomologiczne*. **57**: 3–207.

Bremer, K. (1994) Branch support and tree stability. *Cladistics* **10**: 295–304.

da Silva, M.J. (2010) Filogenia e biogeografia de *Lonchocarpus* s.l. e revisão taxonômica dos gêneros *Muellera* L.f. e *Dahlstedtia* Malme (Leguminosae, Papilionoideae, Millettieae). Tese de Doutorado, Campinas, Universidade Estadual de Campinas, Brazil.

da Silva, M.J., de Queiroz, L.P., Tozzi, A.M.G.D.A., Lewis, G.P. & de Sousa, A.P. (2012) Phylogeny and biogeography of *Lonchocarpus* sensu lato and its allies in the tribe Millettieae (Leguminosae, Papilionoideae). *Taxon* **61**: 93–108.

da Silva, M.J. & Tozzi, A.M.G.D.A. (2012) Taxonomic revision of *Lonchocarpus* s. str. (Leguminosae, Papilionoideae) from Brazil. *Acta Botanica Brasilica* **26**: 357–377.

Debry, R.W. (2001) Improving interpretation of the decay index for DNA sequence data. *Systematic Biology* **50**: 742–752.

Delobel, A., Anton, K-W, Le Rü, B. & Kergoat, G.J. (2013) Morphology, biology and phylogeny of African seed beetles belonging to the *Bruchidius ituriensis* species group (Coleoptera: Chrysomelidae: Bruchinae). *Genus - International Journal of Invertebrate Taxonomy* **24**: 39–63.

Erixon, P., Svennblad, B., Britton, T. & Oxelman, B. (2003) Reliability of Bayesian posterior probabilities and bootstrap frequencies in phylogenetics. *Systematic Biology* **52**: 665–673.

Felsenstein, J. (1985) Confidence limits on phylogenies with a molecular clock. *Systematic Zoology* **34**: 152–161.

Forey, P.L. & Kitching, I.J. (2000) Experiments in coding multistate characters. In: Scotland, R.W. & Pennington, T. (Eds.), Homology and Systematics: Coding Characters for Phylogenetic Analysis. Taylor & Francis, London, pp. 54–80.

Goloboff, P.A., Farris, J.S. & Nixon, K.C. (2008) TNT, a free program for phylogenetic analysis. *Cladistics* **24**: 774–786.

Goloboff, P.A., Farris, J.S., Källersjö, M., Oxelmann, B., Ramírez, M.J. & Szumik, C.A. (2003) Improvements to resampling measures of group support. *Cladistics* **19**: 324–332.

Haines, M.L., Martin, J.-F., Emberson, R.M., Syrett, P., Withers, T.M. & Worner, S.P. (2007) Can sibling species explain the broadening of the host range of the broom seed beetle, *Bruchidius villosus* (F.) (Coleoptera: Chrysomelidae) in New Zealand? *New Zealand Entomologist* **30**: 5–11.

Hetz, M. & Johnson, C.D. (1988) Hymenopterous parasites of some bruchid beetles of North and Central America. *Journal of Stored Products. Research*. **24**:131–143.

Hillis, D.M. & Bull, J.J. (1993) An empirical test of bootstrapping as a method for assessing confidence in phylogenetic analysis. *Systematic Biology* **42**: 182–192.

ICZN (1999) International Code of Zoological Nomenclature, fourth edition [online version]. The International Trust for Zoological Nomenclature, London, xxix + 1–306. Available from: http://www.nhm.ac.uk/hosted-sites/iczn/code/ (accessed 11 May 2016).

Janzen, D.H. (1975). Interactions of seeds and their insect predators/parasitoids in a tropical deciduous forest. In *Evolutionary strategies of parasitic insects and mites* (pp. 154–186). Springer US.

Janzen, D.H. (1977) The interaction of seed predators and seed chemistry. In: Labeyrie, V. (Ed.), Comportement des Insectes et Milieu Trophique. Vol. 265. Colloques Internationaux du Centre National de la Recherche Scientifique, Paris, pp. 415–428.

Janzen, D.H. (1978) The ecology and evolutionary biology of seed chemistry as relates to seed predation. In: Harborne, J.B. (Ed.), Biochemical Aspects of Plant and Animal Coevolution. Elsevier Academic Press, London, pp. 163–206.

Janzen, D.H. (1980) Specificity of seed-attacking beetles in a Costa Rican deciduous forest. *Journal of Ecology*. : 929–952.

Kass, R.E. & Raftery, A.E. (1995) Bayes factors. *Journal of the American Statistical Association* **90**: 773–795.

Kato, T., Bonet, A., Yoshitake, H., Romero-Nápoles, J., Jinbo, U., Ito, M. & Shimada, M. (2010) Evolution of host utilization patterns in the seed beetle genus *Mimosestes* Bridwell (Coleoptera: Chrysomelidae: Bruchinae). *Molecular Phylogenetics and Evolution* **55**: 816–832.

Kergoat, G.J., Alvarez, N., Hossaert-McKey, M., Faure, N. & Silvain, J.-F. (2005a) Parallels in the evolution of the two largest New and Old World seed-beetle genera (Coleoptera, Bruchidae). *Molecular Ecology* **14**: 4003–4021.

Kergoat, G.J., Delobel, A., Fédière, G., Le Rü, B. & Silvain, J.-F. (2005b) Both host-plant phylogeny and chemistry have shaped the African seed-beetle radiation. *Molecular Phylogenetics and Evolution* **35**: 602–611.

Kergoat, G.J., Delobel, A., Le Ru, B. & Silvain, J.-F. (2008) Seed beetles in the age of the molecule: recent advances on systematics and host-plant association patterns. In: Jolivet, P., Santiago-Blay, J. & Schmitt, M. (Eds.), Researches on Chrysomelidae Volume 1. Brill, Leiden, the Netherlands, pp. 59–86.

Kergoat, G.J., Delobel, A. & Silvain, J.-F. (2004) Phylogeny and host-specificity of European seed beetles (Coleoptera, Bruchidae), new insights from molecular and ecological data. *Molecular Phylogenetics and Evolution* **32**: 855–865.

Kergoat, G.J., Le Ru, B.P., Genson, G., Cruaud, C., Couloux, A. & Delobel, A. (2011) Phylogenetics, species boundaries and timing of resource tracking in a highly specialized group of seed beetles (Coleoptera: Chrysomelidae: Bruchinae). *Molecular Phylogenetics and Evolution* **59**: 746–760.

Kergoat, G.J., Le Ru, B., Sadeghi, S.E., Tuda, M., Reid, C.A., György, Z., Genson, G., Ribeiro-Costa, C.S. & Delobel, A. (2015) Evolution of *Spermophagus* seed beetles (Coleoptera, Bruchinae, Amblycerini) indicates both synchronous and delayed colonizations of host plants. *Molecular Phylogenetics and Evolution* **89**: 91–103.

Kergoat, G.J. & Silvain, J.-F. (2004) Le genre *Bruchidius* (Coleoptera: Bruchidae) est-il monophylétique? Apports des méthodes de parcimonie, maximum de vraisemblance et inférence bayésienne. In: Bourgoin, T. & Silvain, J.-F. (Eds.), Avenir et pertinence des méthodes d'analyses en phylogénie moléculaire. Volume 22 de Biosystema. Société française de Systématique, Paris, pp. 113–125.

Kergoat, G.J., Silvain, J.-F., Buranapanichpan, S. & Tuda, M. (2007a) When insects help to resolve plant phylogeny: evidence for a paraphyletic genus *Acacia* from the systematics and host-plant. *Zoologica Scripta* **36**: 143–152.

Kergoat, G.J., Silvain, J.-F., Delobel, A., Tuda, M. & Anton, K.-W. (2007b) Defining the limits of taxonomic conservatism in host-plant use for phytophagous insects: molecular systematics and evolution of host-plant associations in the seed-beetle genus *Bruchus* Linnaeus (Coleoptera: Chrysomelidae: Bruchinae). *Molecular Phylogenetics and Evolution* **43**: 251–269.

Kingsolver, J.M. (1970) Study of male genitalia in Bruchidae (Coleoptera). *Proceedings of the Entomological Society of Washington* **72**: 370–386.

Kingsolver, J.M. & Whitehead, D.R. (1974a) Biosystematics of Central American species of *Ctenocolum*, a new genus of seed beetles (Coleoptera: Bruchidae). *Proceedings of the Biological Society of Washington* **87**: 283–312.

Kingsolver, J.M. & Whitehead, D.R. (1974b) Classification and comparative biology of the seed beetle genus *Caryedes* Hummel (Coleoptera: Bruchidae). *Transactions of the American Entomological Society* **100**: 341–436.

Kingsolver, J.M. (1990) New World Bruchidae past, present, future. In: Fujii, K., Gatehouse, A.M.R., Johnson, C.D., Mitchel, R. & Yoshida, T. (Eds.), Bruchids and Legumes: Economics, Ecology and Coevolution. Springer, Netherlands, pp. 121–129.

Lawrence, J.F., Beutel, R.G., Leschen, R.A.B. & Ślipiński, A. (2010) Glossary of morphological terms. In: Leschen, R.A.B., Beutel, R.G. & Lawrence, J.F. (Eds.), Handbook of Zoology. Vol. 2. Morphology and Systematics (Elateroidea, Bostrichformia, Cucujiformia partim). Walter de Gruyter, Berlin, pp. 9–20.

Lewis, P.O. (2001) A likelihood approach to estimating phylogeny from discrete morphological character data. *Systematic Biology* **50**: 913–925.

Luca, Y. de (1972) Catalogue raisonné des insectes des Antilles francaises. Coleoptera: Bruchidae. *Annales de zoologie: Ecologie animale* **4**: 103–107.

Maddison, W.P. & Maddison, D.R. (2017) Mesquite: a modular system for evolutionary analysis. Version 3.2 http://mesquiteproject.org.

Manfio, D., Ribeiro-Costa, C.S. & Caron, E. (2013) Phylogeny and revision of the New World seed-feeding bruchine genus *Gibbobruchus* Pic (Coleoptera: Chrysomelidae). *Invertebrate Systematics* **27**: 1–37.

Manfio, D. & Ribeiro-Costa, C.S. (2016) A key to American genus *Merobruchus* Bridwell (Coleoptera: Chrysomelidae: Bruchinae) with descriptions of species and two new host plant records for the subfamily. *Zootaxa* **4078**: 284–319.

Manfio, D., Jorge, I.R., Morse, G.E. & Ribeiro-Costa, C.S. (2016) The New World *Gibbobruchus* Pic (Coleoptera, Chrysomelidae, Bruchinae): description of a new species and phylogenetic insights into the evolution of host associations and biogeography. *Zootaxa* **4103**: 513–525.

Morrone, J.J. (2014) Biogeographical regionalisation of the Neotropical region. *Zootaxa* **3782**: 1–110.

Morse, G. (2014) Bruchinae Latreille, 1802. In: Leschen Richard, A.B. & Beutel, R.G. (Eds.), Handbook of Zoology. Volume **3**: Morphology and systematics (Chrysomeloidea, Curculionoidea). De Gruyter, Berlin, pp. 189–196.

Morse, G.E. & Farrell, B.D. (2005a) Ecological and evolutionary diversification of the seed beetle genus *Stator* (Coleoptera: Chrysomelidae: Bruchinae). *Evolution* **59**: 1315–1333.

Morse, G.E. & Farrell, B.D. (2005b) Interspecific phylogeography of the *Stator limbatus* species complex: the geographic context of speciation and specialization. *Molecular Phylogenetics and Evolution* **36**: 201–213.

Nápoles, J.R., Ayers, T.J. & Johnson, C.D. (2002) Cladistics, Bruchids and host plants: evolutionary interactions in *Amblycerus* (Coleoptera: Bruchidae). *Acta Zoológica Mexicana* **86**: 1–16.

Nixon, K.C. (1999–2002) Winclada, Version 1.00.08. Published by the author, Ithaca, New York, NY. Available from: http://www.cladistics.com/ (Accessed May 2016).

Ratcliffe, B.C. (2013) Best writing and curatorial practices for describing a new species of beetle: a primer. *The Coleopterists Bulletin* **67**: 107–113.

Romero, N.J. (2016). Escarabajos (Coleoptera: Bruchidae) asociados a semillas del género *Piscidia* L., 1759 (Leguminosae). *Acta Zoológica Mexicana (n.s.)* **32**: 286–295.

Romero, N.J. & Westcott, R.L. (2011) The Bruchidae (Insecta: Coleoptera) of La Reserva de la Biósfera Sierra de Huautla, Morelos, Mexico, with descriptions of two new species and an annotated checklist. *Insecta Mundi* **166**: 1–15.

Ronquist, F., Teslenko, M., van der Mark, P., Ayres, D.L., Darling, A., Höhna, S., Larget, B., Liu, L., Suchard, M.A. & Huelsenbeck, J.P. (2012) MrBayes 3.2: efficient Bayesian phylogenetic inference and model choice across a large model space. *Systematic Biology* **61**: 539–542.

Sari, L.T., Ribeiro-Costa, C.S. & Medeiros, A.C.S. (2002) Insects associated with seeds of *Lonchocarpus muehlbergianus* Hassl. (Fabaceae) in Três Barras, Paraná, Brazil. *Neotropical Entomology* **31**: 483–486.

Silva, J.A.P. & Ribeiro-Costa, C.S. (2008) Morfologia comparada dos gêneros do grupo *Merobruchus* (Coleoptera: Chrysomelidae: Bruchinae): diagnoses e chave. *Revista Brasileira de Zoologia* **25**: 802–826.

Silvain, J.-F. & Delobel, A. (1998) Phylogeny of West African *Caryedon* (Coleoptera: Bruchidae): congruence between molecular and morphological data. *Molecular Phylogenetics and Evolution* **9**: 533–541.

Slove, J. & Janz, N. (2011) The Relationship between diet breadth and geographic range size in the butterfly subfamily Nymphalinae – a study of global scale. *PLoS One* **6**: e16057.

Tuda, M., Rönn, J., Buranapanichpan, S., Wasano, N. & Arnqvist, G. (2006) Evolutionary diversification of the bean beetle genus *Callosobruchus* (Coleoptera: Bruchidae): traits associated with stored-product pest status. *Molecular Ecology* **15**: 3541–3551.

Whitehead, D.R. & Kingsolver, J.M. (1975) Biosystematics of the North and Central American species of *Gibbobruchus* (Coleoptera: Bruchidae: Bruchinae). *Transactions of the American Entomological Society* **101**: 167–225.

Wink, M. (2013) Evolution of secondary metabolites in legumes (Fabaceae). *South African Journal of Botany* **89**: 164–175.

Wunderlin, R.P. 2010. New combinations in *Schnella* (Fabaceae: Caesalpinioideae: Cercideae). *Phytoneuron* **49**: 1–5.

Zacher, F. (1952) Die Nährpflanzen der Samenkäfer. *Zeitschrift für angewandte Entomologie* **33**: 460–480.

Appendix 1. Data matrix for *Ctenocolum*. (–) inapplicable state; (?) missing data; [ ] polymorphic state.

Species/ Characters	0	0	0	0	0	0	0	0	0	1	1	1	1	1	1	1	1	1	1	2	2	2	2	2	2	2	2	2	2	3	3	3	3	3	3	3	3	3	4	4	4
	1	2	3	4	5	6	7	8	9	0	1	2	3	4	5	6	7	8	9	0	1	2	3	4	5	6	7	8	9	0	1	2	3	4	5	6	7	8	9	0	1	2
Pachymerus cardo	0	1	0	-	1	1	1	0	0	0	0	0	1	-	0	1	0	2	0	0	0	0	0	0	-	0	1	0	0	0	0	0	0	-	-	-	0	1	0	1	-	2/3
Pygiopachymerus lineola	0	1	1	0	0	0	-	0	0	1	1	0	1	1	0	1	1	2	0	0	0	0	-	0	-	0	0	0	0	0	0	0	0	0	-	1	0	0	1	1	0	?	2/3
Meibomeus funebris	0	0	0	0	0	1	0	0	0	0	1	1	0	0	0	0	1	0	1	1	0	0	0	1	1	1	1	1	1	0	0	1	0	-	0	-	0	1	0	0	8	2/3
Meibomeus petrolinae	0	0	0	0	0	0	-	0	0	0	0	1	0	0	0	0	1	0	1	1	0	0	0	1	1	1	1	0	1	0	0	1	0	-	0	-	0	1	0	0	8	2/3
Caryedes brasiliensis	0	1	1	0	1	0	-	1	0	0	0	0	0	0	0	0	0	2	0	1	0	0	0	1	1	1	1	1	0	0	0	1	0	-	0	-	0	0	-	0	7	2/3
Caryedes quadridens	0	1	1	0	1	1	1	1	1	1	1	1	0	0	0	0	0	2	?	1	1	0	0	1	0	1	1	1	0	0	0	1	0	-	0	-	0	0	-	0	2	2/3
C. tuberculatum	1	0	1	1	1	1	1	0	1	1	1	1	1	1	0	1	1	2	0	1	0	1	0	1	1	1	0	0	1	1	0	1	0	-	1	1	1	1	1	0	6	2
C. inmaculatus	1	0	1	1	1	1	1	0	1	1	1	1	1	1	0	1	1	2	0	1	0	1	0	1	1	1	0	0	1	1	0	1	0	-	1	1	1	1	1	?	?	2
sp. n.																																									
C. janzeni	1	1	1	1	1	1	1	0	1	1	1	0	1	1	1	1	1	2	0	1	0	1	0	1	0	1	0	0	1	1	0	1	0	-	1	0	1	1	1	0	3/6	0/1/2
C. acapulcensis	1	1	1	1	1	1	1	0	1	1	1	0	1	0	0	1	1	2	0	1	0	1	0	1	0	1	0	0	1	1	0	1	0	-	1	0	1	1	1	0	3	2
C. salvini	1	1	1	1	1	1	1	0	1	1	1	0	1	1	1	1	1	2	0	1	0	1	0	1	0	1	0	0	1	1	0	1	0	-	1	0	1	1	1	?	1	2
C. punctinotatus	1	0	1	0	1	1	0	0	1	1	1	1	1	1	0	0	0	1	1	1	1	1	1	1	1	1	0	0	1	0	1	1	1	1	1	1	1	1	1	?	?	2
C. pygospilotus	1	0	1	0	1	1	0	0	1	1	1	1	1	1	0	0	0	1	1	1	1	1	1	1	1	1	0	0	1	0	1	1	1	1	1	1	1	1	1	?	3	1
C. colburni	1	0	1	0	1	1	0	0	1	1	1	1	1	1	0	0	0	1	1	1	1	1	1	1	1	1	0	0	1	0	1	1	1	0	1	1	1	1	1	?	6	2
C. pallidus **sp. n.**	1	1	1	0	1	1	0	0	1	1	1	1	1	1	0	0	0	1	1	1	1	1	1	1	1	1	0	0	1	0	1	1	1	0	1	1	1	1	1	0	4	2
C. podagricus	1	0	1	0	1	1	0	0	1	1	1	1	1	1	0	0	0	1	1	1	1	1	1	1	1	1	0	0	1	0	1	1	1	1	1	1	1	1	1	1	0/3/6	1/2/3
C. milelo	1	0	1	0	1	1	0	0	1	1	1	1	1	1	0	0	0	1	1	1	1	1	1	1	1	1	0	0	1	0	1	1	1	1	1	1	1	1	1	1	5/6	3
C. triangulatus	1	0	1	0	1	1	0	0	1	1	1	1	1	1	0	0	0	1	1	1	1	1	1	1	0	1	0	0	1	0	1	1	1	1	1	1	0	1	1	?	?	2
C. nigronotus	1	0	1	1	1	1	0	0	1	1	1	1	1	1	0	0	0	1	1	1	1	1	1	1	1	1	0	0	1	0	1	1	1	1	1	1	1	1	1	?	3	2
sp. n.																																									
C. aquilus	1	0	1	1	1	1	0	0	1	1	1	1	1	1	0	0	0	1	1	1	1	1	1	1	1	1	0	0	1	0	1	1	1	0	1	1	1	1	1	1	5	3
C. biolleyi	1	0	1	0	1	1	0	0	1	1	1	1	1	1	0	0	0	1	1	1	1	1	1	1	1	1	0	0	1	0	1	1	1	0	1	1	1	1	1	1	6	2
C. martiale	1	0	1	0	1	1	0	0	1	1	1	1	1	1	0	0	0	1	1	1	1	1	1	1	1	1	0	0	1	0	1	1	1	0	1	1	1	1	1	1	6	2